Journal of Human Evolution 176 (2023) 103312

Contents lists available at ScienceDirect

Journal of Human Evolution

journal homepage: www.elsevier.com/locate/jhevol

Reconstructing the provenance of the hominin fossils from Trinil (Java, Indonesia) through an integrated analysis of the historical and recent excavations

Eduard Pop [a, b, *], Sander Hilgen [a, c], Shinatria Adhityatama [d], Harold Berghuis [b], Tom Veldkamp [e], Hubert Vonhof [f], Indra Sutisna [g], Gerrit Alink [b], Sofwan Noerwidi [h], Wil Roebroeks [b], Josephine Joordens [a, b, c, i]

[a] Naturalis Biodiversity Center, P.O. Box 9517, 2300 RA, Leiden, the Netherlands
[b] Faculty of Archaeology, Leiden University, P.O. Box 9514, 2300 RA, Leiden, the Netherlands
[c] Faculty of Science, Vrije Universiteit, de Boelelaan 1085, 1081 HV, Amsterdam, the Netherlands
[d] Griffith Centre for Social and Cultural Research, Griffith University, Gold Coast Campus, 58 Parklands Drive, Southport, Qld, 4222, Australia
[e] Faculty ITC, University of Twente, P.O. Box 217, 7500 AE, Enschede, the Netherlands
[f] Max Planck Institute for Chemistry, Hahn-Meitner-Weg 1, 55128, Mainz, Germany
[g] Geological Museum, Jl. Diponegoro 57, Bandung, Jawa Barat, 40122, Bandung, Indonesia
[h] Pusat Riset Arkeometri, Organisasi Riset Arkeologi, Bahasa, dan Sastra, Badan Riset dan Inovasi Nasional (OR ARBASTRA — BRIN), Jl. Condet Pejaten 4, Ps. Minggu, Jakarta Selatan, DKI Jakarta, 12510, Indonesia
[i] Faculty of Science and Engineering, Maastricht University, Paul-Henri Spaaklaan 1, 6229 EN, Maastricht, the Netherlands

ARTICLE INFO

Article history:
Received 24 December 2021
Accepted 17 December 2022
Available online xxx

Keywords:
Homo erectus
Stratigraphy
Dubois Collection
Pleistocene Indonesia
Geographic information system

ABSTRACT

In the early 1890s at Trinil, Eugène Dubois found a hominin skullcap (Trinil 2) and femur (Trinil 3, Femur I), situated at the same level ca. 10–15 m apart. He interpreted them as representing one species, *Pithecanthropus erectus* (now *Homo erectus*) which he inferred to be a transitional form between apes and humans. Ever since, this interpretation has been questioned—as the skullcap looked archaic and the femur surprisingly modern. From the 1950s onward, chemical and morphological analyses rekindled the debate. Concurrently, (bio)stratigraphic arguments gained importance, raising the stakes by extrapolating the consequences of potential mixing of hominin remains to the homogeneity of the complete Trinil fossil assemblage. However, conclusive evidence on the provenance and age of the hominin fossils remains absent. New Trinil fieldwork yielded unmanned aerial vehicle imagery, digital elevation models, and stratigraphic observations that have been integrated here with an analysis of the historical excavation documentation. Using a geographic information system and sightline analysis, the position of the historical excavation pits and the hominin fossils therein were reconstructed, and the historical stratigraphy was connected to that of new sections and test pits. This study documents five strata situated at low water level at the excavation site. Cutting into a lahar breccia are two similarly oriented, but asynchronous pre-terrace fluvial channels whose highly fossiliferous infills are identified as the primary targets of the historical excavations (Bone-Bearing Channel 1, 830–773 ka; Bone-Bearing Channel 2, 560–380 ka), providing evidence for a mixed faunal assemblage and yielding most of the hominin fossils. These channels were incised by younger terrace-related fluvial channels (terminal Middle or Late Pleistocene) that directly intersect the historical excavations and the reconstructed discovery location of Femur I, thereby providing an explanation for the relatively modern morphology of this 'bone of contention'. The paleoanthropological implications are discussed in light of the current framework of human evolution in Southeast Asia.

* Corresponding author.
E-mail address: eduard.pop@naturalis.nl (E. Pop).

https://doi.org/10.1016/j.jhevol.2022.103312

1. Introduction

In 1887, the Dutch physician Eugène Dubois joined the Dutch army for service in the Dutch East Indies, as he was convinced that fossils of the 'missing link' between humans and apes could be found in the tropics. After unfruitful searches on Sumatra and in cave sites on Java, he started excavations in 1891 at Trinil (Fig. 1A–C; Dubois, 1892a), stimulated by the earlier recovery of large amounts of fossils in that area of the Solo River by the Javanese painter and scholar Raden Saleh. Fossil assemblages were initially recovered from bone beds in two 'sandstone plates' sticking out from both shores of the Solo River. Among the rich faunal material (see Dubois, 1907, 1908), a hominid molar (Trinil 1) was found on the left bank (Fig. 1D; Dubois, 1892a). The discovery of a hominin skullcap (Trinil 2; Fig. 1D) one meter from the molar made him decide to excavate extensively at Trinil and try to obtain more elements of this possible 'transitional form' (Dubois, 1892b). He was successful, insofar that a year later his army sergeants Kriele and de Winter—Dubois was normally working on the fossils at Tulung Agung, 100 km southeast of Trinil (Theunissen, 1990)—found a human-like femur (Trinil 3; Dubois, 1893a), 10–15 m away from but at the same level as the skullcap (Dubois, 1894a, 1894b, 1932a, 1934), and in 1892, a second molar (Trinil 4; Fig. 1D). Dubois subsequently attributed all these fossils to the species *Pithecanthropus erectus* (Dubois, 1894a, 1896a), which was later subsumed into *Homo erectus* (Mayr, 1944, 1950).

The Trinil hominin fossils have not only played a critical role in understanding human evolution and in the development of paleoanthropology as a research field, but also sparked intense debates that started directly after his discoveries (see section 1.1 below; e.g., Theunissen 1990). These debates particularly dealt with the question of whether the archaic-looking skullcap and surprisingly modern femur (Femur I) belonged to the same species (see Howell, 1994 for the position of Dubois' contemporaries). The long publication record on this subject shows that these debates flare up regularly—up to the present—and in some cases with a fervor similar to that of Dubois' days. The focus of the debates in the last fifty years has, however, broadened, questioning not only the hominin fossils but also the stratigraphy of the site itself, the homogeneity of the Trinil collections, and the position of Trinil within the biostratigraphy of Java (e.g., de Vos et al., 1982; Bartstra, 1983; Sondaar et al., 1983). The debates clearly illustrate the importance of the Trinil site for both paleoanthropology and paleontology. However, conclusive evidence regarding the provenance of the hominin (and other) fossils and the possible occurrence of stratigraphic mixing has not been presented thus far. By integrating the results of new fieldwork at and around Trinil (see also Hilgen et al., 2023) with a detailed analysis of the historical documentation of this site, this study aims to provide the data necessary to solve most of the ongoing disputes and assess the implications of the conclusions drawn.

1.1. Research history following Dubois' discovery

The key hominin fossils from Trinil, the skullcap, Femur I, and molars (Fig. 1D)—which Dubois considered to be from the same species *Pithecanthropus erectus* and even the same individual (Dubois, 1892a)—were extensively covered in a series of publications that particularly focused on their morphology (Dubois, 1894a, 1895a, 1895b, 1895c, 1896b, 1896c, 1896d, 1896e, 1896f). From the first publication onward, contemporaries of Dubois expressed doubts regarding the archaic-looking skullcap belonging to the same species as the femur (Femur I), which was seen as very modern in its appearance (e.g., Cunningham, 1895; Manouvrier, 1895; Hepburn, 1896). These debates mostly focused on the

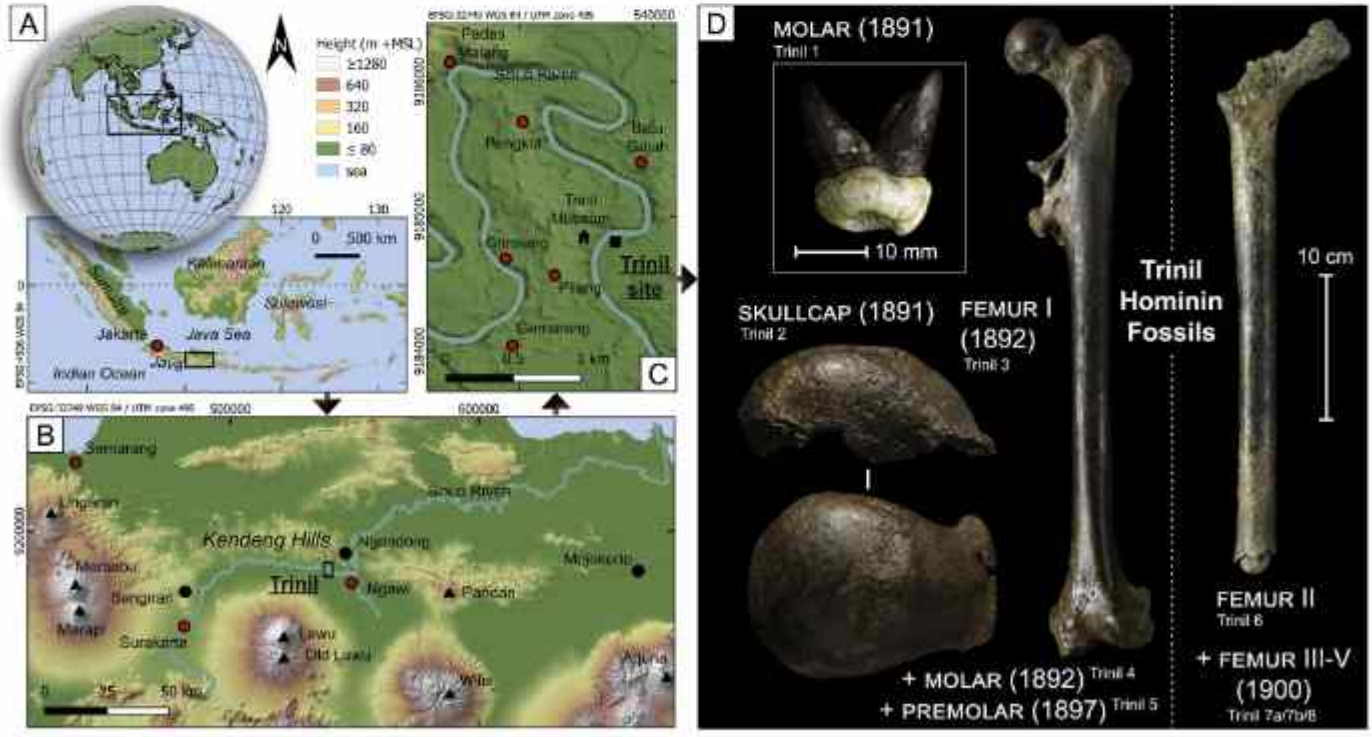

Figure 1. Location of the Trinil site on Java, in Indonesia (**A**), within Middle/East Java (**B**); other key fossil-bearing sites along the Solo River (black dots), major cities (red dots), and volcanoes (triangles) are also indicated. (**C**) The Solo River meander near Trinil with the site/museum and nearby villages (red dots); (**D**) Key fossils found by Dubois at Trinil: the skullcap and molar found in 1891, the femur found in 1892 (Femur I), and the most complete femur (Femur II) from the ones excavated in 1900 (Femora II–V). The Femora II–V were only recognized as being hominin in 1932–1933. The Trinil numbers (i.e., Trinil 1–8) are conform with Indriati (2004). (For interpretation of the references to color in this figure legend, the reader is referred to the Web version of this article.)

morphology and taxonomy of the fossils (see Theunissen, 1990 for a comprehensive review). In response to the critique and to prove the contemporaneity of the hominin fossils, Dubois provided somewhat more information on the stratigraphy of Trinil, the provenance of the fossils, and their similar degree of fossilization (e.g., Dubois, 1896a). The debate continued, again largely on morphological grounds (but see Hrdlicka, 1930), and gradually, the views on Dubois' thesis became more favorable (Theunissen, 1990). The excavations at the left bank of the Solo River continued—with interruptions in 1894 and 1898—until 1900 (de Vos and Aziz, 1989). Except for a premolar found in 1897 (Dubois, 1899), these excavations yielded no further hominin remains. However, in 1932, four more hominin femora (Trinil 6, 7a/b, 8 or Femora II–V; see Femur II in Fig. 1D) were discovered in previously unopened boxes of the Dubois collection (currently stored at Naturalis Biodiversity Center, Leiden, the Netherlands) said to have come from the 1900 excavations at Trinil (Dubois, 1932a, 1932b, 1934).

The Trinil excavations led by the German scientist and feminist-pacifist Lenore Selenka in 1907–1908 did not yield any additional hominin fossils but were carried out with more regard for (stratigraphic) provenance and context. This is reflected in the extensive, edited monograph (Selenka and Blanckenhorn, 1911) outlining the methodology of excavation—e.g., the documentation of quadrant, layer, and orientation for each find (Oppenoorth, 1911)—while also describing the stratigraphy in great detail (Carthaus, 1911a; Dozy, 1911a). Unfortunately, most of their original documentation is lost—most likely due to bombardments/fire during World War II (Beck and Joger, 2018). Also the small-scale fieldwork of the Geological Survey Netherlands Indies in 1930 at Trinil (Oppenoorth, 1932, 1936)—which was never published—yielded no further hominin fossils.

In the 1950s, the chemical analyses of the Trinil hominin fossils suggested a similar Middle Pleistocene age for all the fossils (Bergman and Karsten, 1952). Later, Day and Molleson (1973) compared the Trinil femora with fossil and modern specimens, as well as conducting scanning electron microscopy, computed tomography (CT), and chemical analyses on them. They concluded on anatomical grounds that not only Femur I but also Femur II–V do not differ significantly from those of modern humans, while they regarded the analytical evidence on their age as inconclusive. Using energy dispersive microanalysis, Day later found significant differences in heavy element composition between Femur II–V and Femur I (Day 1984, 1986a, 1986b), explained as a potential difference in provenance and/or age. Kennedy (1983: 614) argued that for Femur II–V, not only "their overall pattern unequivocally allies them with sapient comparative groups" but also noted high robusticity in the distal part of the shaft. Kennedy also emphasized that the taxonomic judgment for Femur I should be withheld due to its pathological nature. Chemical analysis by Matsu'ura (1986) produced similar results for the femora, while the deviation of the skullcap was attributed to contamination.

In the 1980s, de Vos, then curator of the Dubois collection, together with Sondaar, put the fossil fauna of Trinil to the forefront. They redefined the Trinil fauna—as to only consist of material from this site—and restructured the biostratigraphy of Java (de Vos et al., 1982; see also van den Bergh et al., 2001) that was originally established by von Koenigswald (1934, 1935). In a second paper, they emphasized that the Trinil assemblage from the Dubois collection (Trinil fauna) was collected from one (stratigraphic) level, the 'Hauptknochenschicht' (H.K.; de Vos and Sondaar, 1982). In the same issue, Bartstra (1982) challenged this notion on stratigraphic arguments: based on fieldwork, he confirmed earlier observations of the presence of several young (low) terraces along the Solo River (Elbert, 1908), with their fills showing lithologies very similar to those of pre-terrace strata. He suggested that the Dubois and Selenka campaigns must have dug through both older strata as well as younger terrace deposits. This resulted in a somewhat bitter discussion (Bartstra, 1983; Sondaar et al., 1983) with each party using different lines of argumentation, thereby clearly illustrating the stakes of the debate. Soeradi et al. (1985) conducted geological fieldwork at Trinil and concluded—using the old stratigraphic framework (Duyfjes, 1936; see also Berghuis et al., 2021 for a revision) and lacking direct chronological control—that all deposits overlying the lahar deposits belong to the same Kabuh Formation, supporting the de Vos et al. (1982) interpretation of the Trinil stratigraphy.

Based on energy dispersive X-ray analysis chemical analysis, Bartsiokas and Day (1993) suggested that Femur I originates from a different stratigraphic layer than the skullcap and other femora, which they—given Dubois' assertion that both fossils were excavated from the same level—attributed to a westward inclination of the strata. This was countered by later X-ray fluorescence measurements from the outside of the hominin specimens (Joordens et al., 2015), which also repeated Kennedy's (1983) notion that the taxonomic judgment for Femur I should be withheld due to the pathological nature of this specimen. Based on an analysis of the structural and density characteristics obtained using CT, a study from the same year concluded that while Femora II–V can be assigned to *H. erectus*, Femur I does not show any of the characteristics of early *Homo* elsewhere and fits comfortably within *Homo sapiens* (Ruff et al., 2015). They convincingly dismissed the arguments of Kennedy and Day and Molleson for assuming a modern morphology for Femur II–V and attributed the different outcomes of the chemical analyses between Bartsiokas and Day (1993) and Joordens et al. (2015) to the latter measuring the exterior, rather than samples from the interior. Recent studies on the two Trinil molars have resulted in their attribution to *H. erectus* (Smith et al., 2009; Noerwidi et al., 2020), while others attribute them to the hominid *Meganthropus* (Zanolli et al., 2019). As their taxonomic attribution is beyond the scope of this study, the molars will be included when reference is made to the Trinil hominin remains. The latest addition to the extensive literature on Trinil concerns a detailed study of the historical documentation of Dubois' and Selenka's excavations and argues that the skullcap and Femur I have the same stratigraphic provenance (Huffman et al., 2022).

Despite the large number of studies devoted to this topic, the stratigraphic position and age of the fossil fauna—including hominin fossils—excavated at Trinil remains contested. The chemical analyses on the hominin fossils have varying outcomes, but the stratigraphic observations of Bartstra have not been refuted by field observations and the modern appearance of Femur I in comparison to those that can be securely attributed to *H. erectus* still supports the possibility of the presence—and historical excavation—of younger strata at Trinil.

1.2. New Trinil fieldwork and objectives of this study

New fieldwork has been carried out at Trinil in 2016, 2018, and 2019, consisting of geological survey, extensive logging, and sampling of sections dug into the present-day river banks of the Solo, as well as excavating test pits targeting the low-lying remains of find-rich deposits situated 0–2 m above the present-day low water level. The fieldwork has resulted in the publication of a revised, independent stratigraphic framework for the wider Trinil area (Berghuis et al., 2021). That study identified seven terraces—together forming the newly defined Solo Formation—overlying the pre-terrace stratigraphy, which includes the revised/newly defined Pliocene Kalibeng and Pleistocene Padas Malang, Batu Gajah, and Trinil Formations. The southward dipping pre-terrace stratigraphy is truncated by a horizontal erosional contact, i.e., moving southward, the terrace stratigraphy is situated on top of

increasingly younger pre-terrace deposits. Although in that paper, the left-bank part of the Trinil site (i.e., the left-bank historical excavation areas of Dubois and Selenka, from here on simply referred to as 'Trinil site') was not covered in detail; at this locality, T2 terrace deposits directly overlie the pre-terrace deposits; specifically, the lahar breccia assigned to the Batu Gajah Formation (Berghuis et al., 2021; see also Hilgen et al., 2023). The (chrono) stratigraphy of the Trinil site, in particular, is covered in detail by Hilgen et al. (2023).

While these works provide important insights into the complex local stratigraphy and the age of the encountered sediments, it is nevertheless critical to make a connection between the updated (chrono)stratigraphy and the left bank historical excavations by Dubois and Selenka for two important reasons. First of all, the historical excavations yielded a continuous east–west exposure over a total length of ~90 m—regrettably facilitated by the use of forced labor under a harsh colonial system—whereas the 2018–2019 sections only provide eight 1–2 m wide stratigraphic 'peepholes'. Photos of the historical sections provide insights into the large-scale stratigraphy and its lateral development and also document deposits that were either removed in subsequent excavation seasons or deposits that could not be sufficiently exposed during the 2018–2019 fieldwork. Second, it is critical to understand where the historical excavation pits and the (hominin) fossils found in them were situated in relation to (extant) stratigraphic reference points, particularly where abrupt lateral changes in the stratigraphy are documented.

The objectives of this study, therefore, are to (1) reconstruct the spatial position of the historical, left-bank excavation pits (1891–1908) as well as the spatial position of the hominin fossils found within them, in relation to the remains of the historical excavation site still visible at the present day (Sections 3.1–3.3) and (2) obtain stratigraphic data from the historical documentation, integrate this with the detailed stratigraphic observations obtained in our 2018–2019 fieldwork, and identify the fossil-bearing deposits targeted by the historical excavations (Sections 3.4–3.6). This involves the study of primary historical sources (i.e., high-resolution historical imagery obtained from scanned glass plate negatives and scaled maps) using sightline analyses and their spatial integration into a geographic information system (GIS) environment, where it can be compared with unmanned aerial vehicle (UAV) imagery/digital elevation models (DEMs) documenting the present-day situation. When the spatial position of the exposures visible in the historical imagery is known, the stratigraphy visible in them can be studied in detail and compared and correlated with the 2018–2019 sections and test pits.

The data presented here, when combined with the results of geochronological analyses obtained for several of the studied sections and outcrops (see Hilgen et al., 2023), make it possible to reconstruct the stratigraphic provenance of the hominin fossils, assess the potential heterogeneity of the larger Trinil collections (see Discussion), and (possibly) offer a 'final resting place' for Femur I as a 'bone of contention'. Finally, the paleoanthropological implications of the findings in light of the current framework of human evolution in Southeast Asia will be discussed, including future research perspectives.

2. Materials and methods

2.1. Analysis of historical data

Historical sources The used documentation of the historical excavations at the (left-bank part of the) Trinil site consists of photos (Supplementary Online Material [SOM] Figs S1–S22) and maps (S23–S28). A subdivision was made between main data and supporting data sources. The basis for this study was provided by the main data, which is included here completely. For practical reasons, the supporting data are included here in partial form only (as specified below). It should be noted that this study neither aims nor claims to provide an exhaustive overview of the complete Dubois and Selenka archives.

The main data concern scaled maps of the left-bank excavations showing reference points still visible at the present day and/or unambiguous reference points shared with other maps and high-quality photos that cover larger parts of the total excavation area. Meeting these criteria are (1) a glass negative of a photo (DUBO0690) taken in 1894 of the 1891–1893 Dubois excavations (SOM Fig. S1); (2) several versions of an unpublished, scaled map of the Dubois excavations in 1900 (SOM Fig. S23) that show the excavation pits that were under excavation at that time as well as two unambiguous reference points, plus the camera positions of the photos specified under source 3; (3) three glass-negatives of photos (DUBO1400/1494/1399; referred to as, respectively, 1900-I, -II, -III) of the Dubois 1900 excavations taken from three different angles (SOM Figs. S4–S7). Together, sources 1–3 cover the years when 8 out of 9 hominin fossils were found. Further included are (4) a surviving map/plan of the Selenka 1907 excavations (SOM Fig. S24)—showing shared features with the 1900 map; (5) a glass negative of a photo (41_0001) of the Selenka 1907 excavations (SOM Figs. S16–S17).

The supporting data concern (1) glass negatives of additional 1907 photos (see SOM Table S1 for details) that could all be spatially interpreted in relation to the main 1907 photo (see glass negative of photo 41_0001); (2) excavation reports from Dubois' sergeants Kriele and de Winter in letter form, covering the period from 1891 to 1900, that also contain various maps and plans documenting (with the exception of one very early 1891 sketch) the excavations of 1897–1900 and that are either lacking a scale, are schematic, lack sufficient extent, or do not show unambiguous reference points (or any combination thereof); (3) publications by Dubois and Selenka—including a crucial map showing the 1891–1893 excavations (SOM Fig. S25B) and photos from Selenka's monograph; (4) a glass negative of a photo taken by van Es in 1926 of the Trinil site (SOM Fig. S22).

The 1894–1900 and 1926 glass negatives, the 1900 map, and de Kriele and de Winter letters are part of the Dubois Archive of the Naturalis Biodiversity Center (Leiden, the Netherlands; see Albers and De Vos, 2010 for more information on the imagery from the Dubois Archive) and were commercially scanned. The 1894–1900 and 1926 glass negatives were scanned on an Epson scanner at 4800 dpi. The 1900 map was scanned on an OS 14000 A1 scanner at 600 dpi. The scans of the glass negatives are included in this paper (see SOM Table S1 for details). The scans of the letters are available on request.

The 1907 glass negatives are part of the Oppenoorth Archive that was gifted by Joke Oppenoorth to Naturalis Biodiversity Center and curated there. These glass negatives were digitized at the Teylers Museum (Haarlem, the Netherlands) using a Canon 1Ds with an EF 100 mm f/2.8 Macro USM lens. The photographs of the relevant 1907 glass negatives are included in this paper (see SOM Table S1 for details). The 1907 map is part of the Selenka archive curated at the Museum für Naturkunde (Berlin, Germany) and was photographed using a Canon Digital IXUS 960 IS. Lens distortion for the 1907 map was corrected for using the visible grid.

Georeferencing map data The 1900 map was georeferenced using (1) shared reference points visible on the map and in the present day, for which the coordinates are known from either differential global positioning system (DGPS) measurement or extracted from referenced orthophotos; (2) scale information included on several versions of the 1900 map; (3) publicly available historical magnetic

declination data indicating the deviation between compass north and true north (Alken et al., 2021) that can be accessed through an online map viewer (NOAA, 2020). The 1907 map covers a substantially smaller area and did not provide direct (i.e., present-day) reference points. It was, therefore, manually fitted (see SOM S1).

Field of view assessment of historical imagery The bidimensional (2D) field of view (FOV) assessment of a photo with a known camera standpoint (i.e., 1900 photos I–III) was performed as follows: the x (horizontal) coordinates in pixels of two reference points (I and II in Fig. 2A) and the midline (usually $X_{max}/2$) were extracted. The vertical component, i.e., the y-coordinate, was ignored because of uncertainties regarding the vertical camera angle of the photos. For the 1900 photos, the latitude/longitude coordinates of the camera positions were extracted from the georeferenced map in QGIS v. 3.16.1 (QGIS.org, 2020), while a rough approximation of the azimuth of the photo (i.e., its midline) could be estimated. Using the real-world coordinates and estimated azimuth of the camera positions as well as the raster coordinates of the reference points and midline, the latter two could, using trigonometry, be projected on a map as points on an imaginary projection plane lying at an arbitrary distance from the camera position (Fig. 2B; in practice, UAV ortho imagery with differential GPS-measured reference points displayed as point data, see below). When the reference points on the projection plane did not line up with the sightline between the camera position and the actual position of a reference point, small adjustments in the position of the midline were carried out. When correct, it produces a scale (x pixels [in the image] = y m [on the projection plane]) for the projection plane.

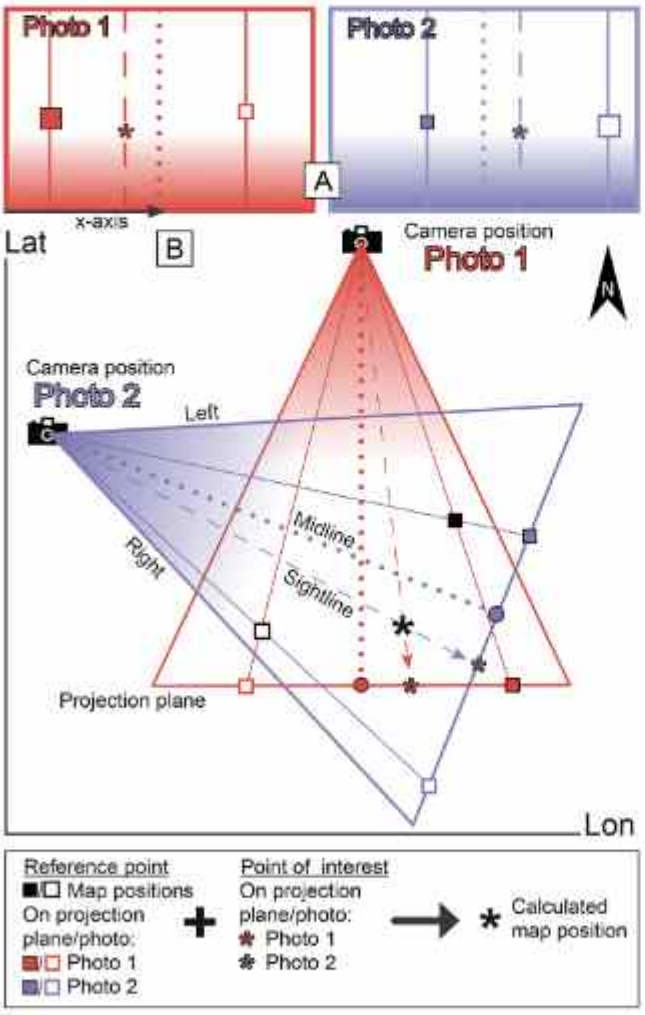

Figure 2. Methodology field of view assessment and sightline intersection analysis for photos with a known camera position. To assess the field of view, the horizontal (x-axis) coordinates of two reference points (I, II; with known map coordinates) and midline (usually $X_{max}/2$) need to be extracted from photo 1 (**A**), which can be projected on an imaginary projection plane lying at an arbitrary distance and (initially) estimated azimuth from the known camera position on the map (**B**). When the sightlines for the reference points do not line up with their projected position on the projection plane, adjustments in the azimuth (midline) are made until they do line up. This same procedure is repeated for photo 2. Now, the (x-axis) coordinate of a point of interest can be extracted from both photos 1 and 2, plotted on the map as sightlines (dashed arrows), with their intersection point providing map coordinates. Abbreviations: Lat – Latitude; Lon – longitude.

For the other photos (i.e., from 1894, 1907), the camera standpoint was not known, making the process of assessing the FOV less straightforward. This involved obtaining a larger number of additional reference/control points; either points with known coordinates obtained through sightline intersections analysis (see below) of two 1900 photos or any combination of 1900 (photo II), 1907, and 1894 photos. Additionally, the intersections of 1894/1900/1907 sightlines with the present-day shoreline were used (as obtained from UAV imagery, see SOM Fig. S29)—assuming no large deviation from the 1900 situation.

For the FOV assessment of the 1894 photo additional control was sought because it documents the 1891–1893 pits yielding key hominin fossils including Femur I. As the photo shows the Kendeng range in the far background, sightlines for this feature were compared with the results of a viewshed analysis from the reconstructed camera position for that photo. For this, the 'GRASS r.viewshed' function in QGIS was used on the publicly available Digital Elevation Model Nasional of Indonesia elevation model (0.27 arcsecond resolution) with default settings, plus the advanced parameters 'consider earth curvature' and 'consider the effect of atmospheric refraction' enabled.

Sightline intersection analysis and complementary functions Having established the FOV for all five photos, real-world coordinates were calculated for features that occur on at least two of these photos (here referred to as sightline intersection analysis). This was done by extracting the raster (x) coordinate for the feature of interest from the first photo and plotting it on the already fixed and scaled projection plane for this photo (Fig. 2B). Together with the camera position, this constitutes a sightline. After repeating this for the same feature visible in the second photo, the latitude/longitude coordinates for a point of interest were calculated by intersecting the two sightlines (Fig. 2B). When a particular feature was only visible on one photo, only an angular orientation could be extracted.

The potential sources of error in the FOV assessment and subsequent sightline intersection analysis could be the result of geometric lens distortion of the images or inaccuracies of the camera positions as indicated on the 1900 map. For the 1900 imagery, it was possible to plot a shared point three times, i.e., once for every image pair; I–II, I–III, II–III. To quantify the spread of the intersections in relation to their arithmetic mean, the root mean square error was calculated for each shared point.

The calculations can also be inversed, allowing the possibility to plot known map features as angular orientations on the historical imagery. This made it possible to plot the locations of the 2018–2019 sections (see Section 2.2) on the back walls visible in the 1900/1907 historical imagery, allowing for direct stratigraphic comparisons at specific points in the historical excavation area.

Furthermore, by adjusting the position of the projection plane (see Fig. 2B) to that of a feature of interest (e.g., a certain position along the back wall), approximate scale bars could be added to the historical imagery. Given the large distance between the camera positions and the features of interest, the effect of potential height

differences between them (i.e., non-level camera position) is negligible. For the 1900 imagery, scale bars along the back wall could be calibrated with each other using the water level within the pit as base level. Direct stratigraphic correlation between the 1900/1907 imagery and the 2018–2019 situation at the east end of the historical excavation area (see section 3.4) made it possible to label the scale bars on the 1900/1907 historical imagery with absolute (but approximate) elevations in m above mean sea level (+MSL).

Stratigraphic analysis of historical imagery All historical imagery outlined in the section Historical sources was carefully inspected for stratigraphic information and geological features. Where necessary, adjustments were made in contrast and brightness/exposure to better recognize layer boundaries and features, which were marked on a separate layer. The thickness of the stratigraphic units could be assessed using the scaling method outlined in the previous section. Although a selection of photos is presented in the main text, all historical imagery can be found in both annotated and unannotated form in the SOM (see SOM Table S1 for details).

2.2. 2018–2019 fieldwork data

Differential global positioning system data The spatial position of sections and reference points for the obtained UAV imagery/DEM were—unless otherwise specified (see below)—measured using a Sokkia GRX2 DGPS. This surveying equipment has a relative positioning accuracy of 3–10 mm horizontally and 5–15 mm vertically. Measurements were taken in the World Geodetic System 84/UTM zone 49S system (EPSG:32749) with elevations recorded as ellipsoidal heights. These were converted to meters m+ MSL by subtracting the local geoid height of 25.142 m obtained from the EGM96 model. From here on all elevations are given as +MSL unless otherwise specified. To account for potential errors in the absolute positioning of the base station and ensure reproducibility in future studies, the coordinates of the center point of the Dubois monument—erected in 1893 to commemorate and indicate the position of his key finds (see SOM Figs. S34 and S35)—is specified here as being: x = 539523.44, y = 9184803.34, z = 87.20 (WGS84; 62.06 m +MSL).

Unmanned aerial vehicle imagery and bathymetric measurements All aerial imagery, which serves as input for both orthorectified images and DEMs (see section below) was collected using a DJI Mavic Pro drone. The overview vertical imagery of the wider Trinil area was taken on 25 September 2018 from an altitude of ca. 120 m. Flying and photography were done using Pix4d v. 4.5.0 software (Pix4d, Prilly). This software, running on a mobile device that is connected to the drone, allows the latter to fly and shoot images of a pre-set area independently. For geographic reference, the internal GPS of the drone was used (in m +MSL).

Aerial imagery of the excavation area was taken on 10 October 2018 from an altitude of ca. 15 m above the low water level of the Solo River using the Pix4d software. The imagery was referenced using ground control points that were marked by spray-painted nails and measured by DGPS (see details above). To reconstruct the surface of the subaqueous parts of the Trinil site, DGPS measurements were taken below water level with the waterproofed module remaining (just) above it, either from a boat or by wading. To best approximate the depth of pits, the DGPS staff was pressed through as much loose mud as possible.

In 2019, work at the excavation area was focused on stratigraphic sections in the present-day river bank and on exposing the more southward lying historical excavation walls of the site. As this area was poorly covered by the 2018 vertical imagery due to overhanging vegetation, additional horizontal and oblique imagery covering this area was manually shot on 11 October 2019. These images were referenced conform to the 2018 imagery.

Orthophoto and digital elevation model generation The UAV imagery was processed using Agisoft Photoscan Professional v. 1.4.5 (Agisoft, 2018), using the reference methods described above. After rendering 3D models from the imagery, they were exported as orthophotos and DEMs (SOM Figs. S29–S32). These were subsequently imported into QGIS for further analysis. This GIS software package was used to combine the 2018 site DEM produced by UAV imagery with the bathymetry measurements taken with DGPS (see above) to create one continuous elevation/bathymetry model (SOM Fig. S31).

Although presented here together in a single map (e.g., Fig. 4), the 2019 river bank DEM was not merged with the 2018 one due to differences in water levels and in excavation progress.

Documentation of sections and test pits and the stratigraphic framework of Trinil The methodology of documenting the sections and the (chrono)stratigraphic work in general is covered in detail by Hilgen et al. (2023). Here the correlations outlined by Hilgen et al. (2023) are used to connect the detailed Trinil site stratigraphy to the formations revised/defined by Berghuis et al. (2021).

Three test pits of 1 m^2 were set out by DGPS in the southeastern part of the historical excavation area where thicker (remnants of) fossil-bearing deposits are preserved above water level. Each started at a different vertical position within the fossil-bearing deposits. The pits and fossil finds within them were carefully excavated, documented, and measured by DGPS (see above). At the end of each season, the stratigraphy of the pit walls was logged and photographed (conform the methodology for sections specified in Hilgen et al., 2023). The fossil finds were plotted vertically on annotated orthophotos to study their vertical distribution.

3. Results

3.1. Spatial reconstruction: Dubois 1900

The results of the spatial reconstruction of the historical excavation pits and the position of the hominin fossils are presented in non-chronological order, starting with the 1900 excavations that yielded the most coherent set of primary documentation.

Georeferencing the 1900 map and field of view assessment of 1900 photos The process of georeferencing the Dubois 1900 map and the assessment of the FOV is described in detail in SOM S1 (see also SOM Figs. S33–S38). Using two clear reference points, scale information, and declination data, the map could successfully be georeferenced (Fig. 3A). Using the camera positions on the 1900 map and three reference points, the FOV's of the three photos could be established (Fig. 3A). A series of points visible on all three photos plots accurately on the 1900 back wall (black triangles in Fig. 3C) with low root mean square errors ranging from 8.7 to 19.4 cm. Other key points along the back wall (Fig. 3B) also plot accurately on the map (Fig. 3C).

Position of the 1900 excavation pit(s) Large parts of the 1900 back wall (as spatially reconstructed in Fig. 3C) are still recognizable in the field today (Fig. 4). The first segment of the wall ran originally from the western end up to platform A, but only the middle part remains visible as it was cut short in the west by a later pit/cut, while toward the east it is covered by rubble. The 2018–2019 Sections S16 and S21 lie in the extension of this first segment, behind (i.e., south of) platforms A and B, respectively. Both platforms were most likely excavated down to water level in 1908 (see below) but the new sections—representing primary deposits—are situated right on the back wall line indicated on the 1900 map. The second segment of the wall is recognizable north of platform A, and runs, after a nudge, straight toward the southeast corner of the 1900 pit on the map. The eastern part of this segment and the southeast corner were not recognized at first due to large blocks of

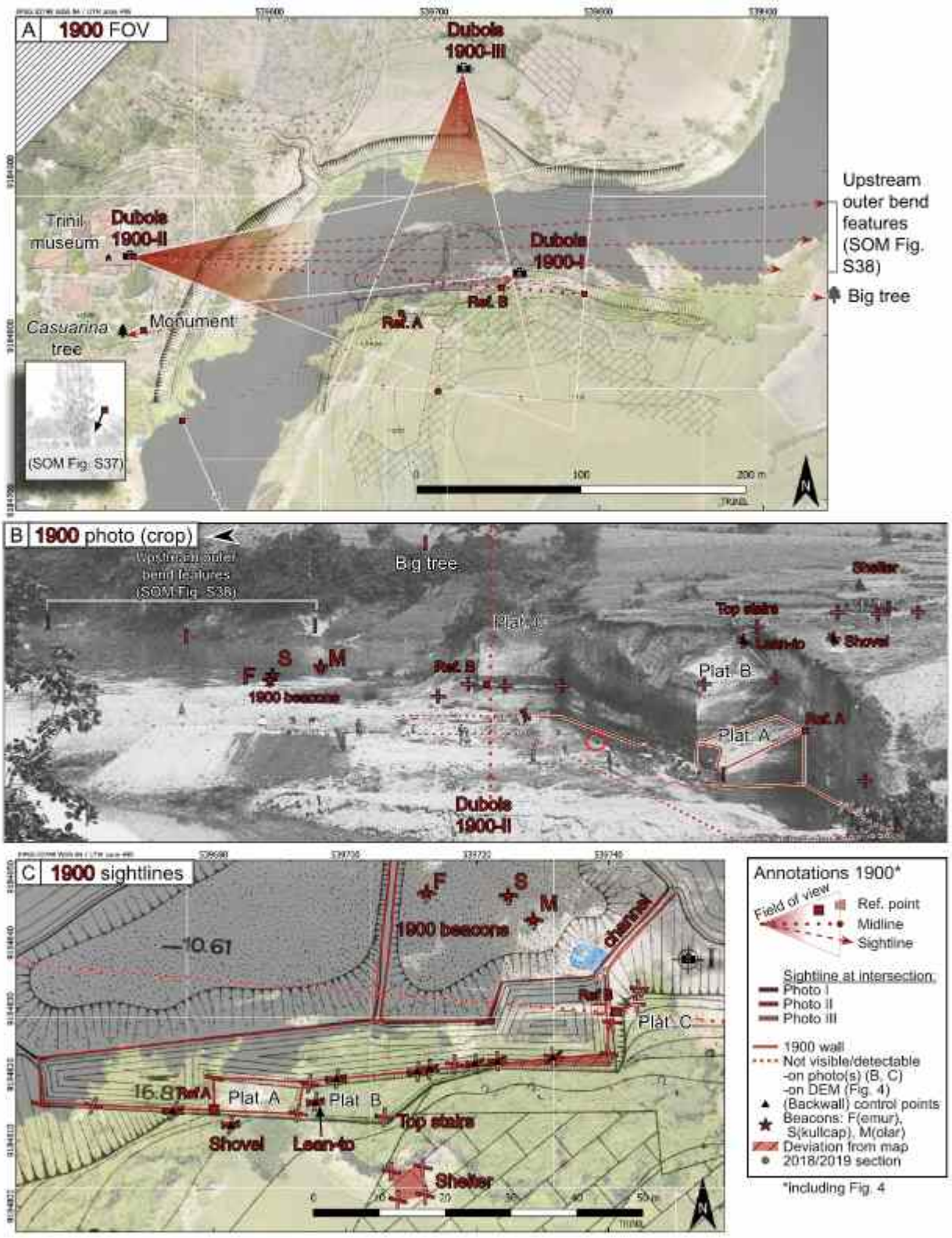

Figure 3. Field of view (FOV) assessment and sightline intersection analysis 1900 imagery. (**A**) Field of view of the three 1900 photos (photos I, II, and III) shown on the georeferenced 1900 map/drone imagery; (**B**) 1900 photo II (cropped) with reference points, 1900 pit outline, and sightline (intersections); (**C**) detailed map with reference points, 1900 pit outline, and sightline (intersections). The close plotting of the sightlines for control points along the back wall (black triangles) suggests low error margins in the reconstructed positions (further confirmed by low root mean square errors, see text). Abbreviation: Ref. = reference point; Plat. = platform.

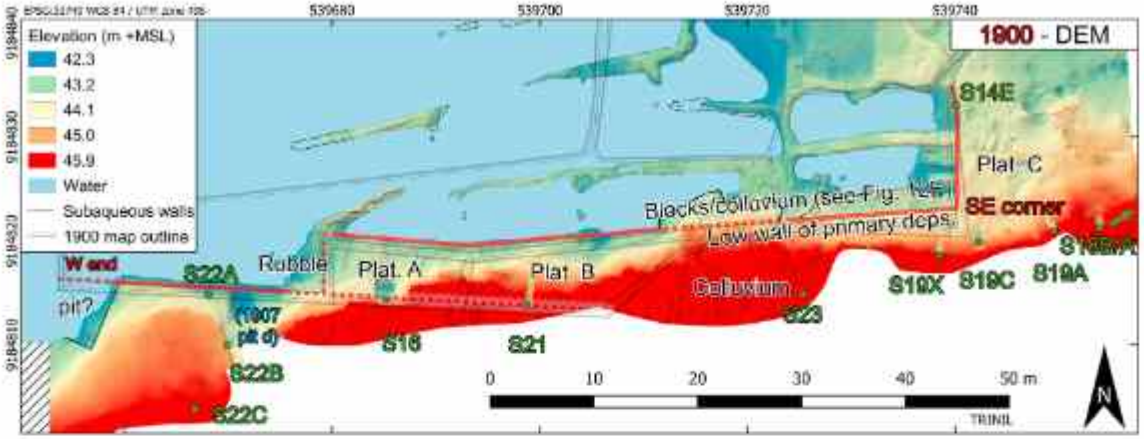

Figure 4. Reconstructing the position of the 1900 pit in relation to the remains visible at the present day, shown as a digital elevation model (DEM). Abbreviation: Plat. = platform.

deposits originating from a higher stratigraphic position lying in front of it (see Section 3.5). Removal of vegetation and colluvium exposed, just south of these blocks, a low, straight wall of primary BBC (Bone-Bearing Channel)-2 deposits (see Section 3.4 and Hilgen et al., 2023) running toward the southeast corner where it meets up with the east wall of the 1900 pit (see also Fig. 9). This suggests a slight deviation of the photo/DEM from the map (hatched area in Fig. 3C). From the southeast corner of the pit, a low wall continues north toward S14E and a characteristic southwest–northeast running (drainage) channel (Fig. 3C). Platform C is completely removed as well, which can be attributed to the 1907/1908 excavations (see below). The northern border of the 1900 pit is on the map situated north of the low walls (former excavation balks) visible in the DEM (Fig. 4); the low walls were probably kept as a buffer or access path between the deep pit and the loose spoils (as suggested by a worker walking there; see red circle on Fig. 3B). The short diagonal wall in the DEM (wavy line in Fig. 4) just north of platform A corresponds to a similar feature just in front of the group of workers in the 1900 photo (Fig. 3B).

Position of hominin fossils (Femora II–V) The fossil Femora II–V are thought to have been excavated in 1900 but were only identified as hominin in 1932 at the museum in Leiden (Dubois, 1932a, 1932b, 1934). Therefore, their position was neither recorded on any map nor reported in the 1900 letters. Dubois mentions a distance of 16–48 m from the skullcap, but given the uncertainty regarding the assumed position of the latter (see below), the femora could originate from anywhere in the nearly 90 m long pit. Nevertheless, their provenance will be further considered in the discussion.

3.2. Spatial reconstruction: Selenka 1907–1908

Field of view assessment of 1907 photo The back wall visible on the Selenka 1907 photo (Fig. 5B) shows partial overlap with that visible on the 1900 photo (Fig. 3B), which made it relatively easy to determine the camera position and FOV of this photo (Fig. 5A). Sightlines of photo features (Fig. 5B) project accurately on the map, for instance, the northwest corner of platform B and the southeast corner of the 1900 excavations (Fig. 5C; see SOM S1 for more details).

Position of the 1907–1908 excavation pits Most of the Selenka field documentation has not been preserved, but a fairly detailed plan of the 1907 excavations is still available (Fig. 5D; see SOM Fig. S24 for original). While generally reflecting the situation visible in the 1907 photo (Fig. 5B), it needed adaptation (Fig. 5D) to fit sightlines obtained from the photo (Fig. 5C) and to connect with the 1900 pit remains identified on the DEM (Fig. 6; see SOM S1 for details).

In the west, pit d of the Selenka map can be clearly recognized, creating a notch in the overlapping Dubois/Selenka back wall (Fig. 6). The line connecting S22A, S16, and S21 (Fig. 6) represents the probable back wall after the 1907/1908 excavations, but in the 1907 photo (Fig. 5B), platform B is still standing. West of platform B, the main Selenka pit (parts a-c) cuts deep into the river bank (Fig. 6), where now predominantly colluvium can be found. At the east end, the back wall runs north toward the southeast corner of the 1900 excavations identified in the field, which is recognizable in the 1907 photo as a slight notch in the wall (Fig. 5B).

As the 1907–1908 excavations were the last large-scale excavations at Trinil, they largely determined the current state of the site, warranting a detailed look at the excavation progress. The part between the 1900 back wall and a–c (Fig. 6) was most likely the source of the blocks lying in front of it. The partially collapsed (i.e., 'decapitated') wall (see Section 3.5 for details) seems to have been removed up to the level of the bone-bearing deposits, after which a track was laid on top of it (Oppenoorth, 1911). Then, excavations were started from the top, which was, judging by the accessory 1907 imagery (SOM Figs. S13–S14), done according to the 1907 plan (i.e., parts a–c). Eventually, a northward extension of the main pit started by Oppenoorth was also excavated to full depth (Carthaus, 1911b), which can only be the area north of A–C. Excluding the surface area covered by the necessary steps in the wall, the complete pit would have measured ~37 × 6 m (222 m^2), which together with pit d (31.5 m^2) totals 253.5 m^2, closely approximating the total excavated area of 260 m^2 reported for 1907 (Oppenoorth, 1911). Preparatory work took place on platform C that year (part e on Fig. 5D; see SOM Fig. S19) but was not described in the report for 1907.

Unfortunately, maps or documentation of the 1908 excavation have not survived, except for a short report (Dozy, 1911b). Particular pits were (again) labeled as a–c, but the map referred to in the report was omitted from the publication. However, part c was described as being situated in the easternmost part of the excavation area where the bone-bearing deposits completely disappear (Dozy, 1911b). This was most likely where preparatory work took place the previous year; i.e., platform C (Fig. 6; part e/'unexcavated' on Fig. 5D). The remaining parts, a and b, may have been the (remains of) platforms A and B, as they are not visible on post-1907 imagery (SOM Figs. S21–S22). Details on fossil finds made there or find density are absent in the documentation.

3.3. Spatial reconstruction: Dubois 1894 (1891–1893)

Field of view assessment of 1894 photo The 1894 photo, documenting a very early stage of the Trinil excavations, does not show

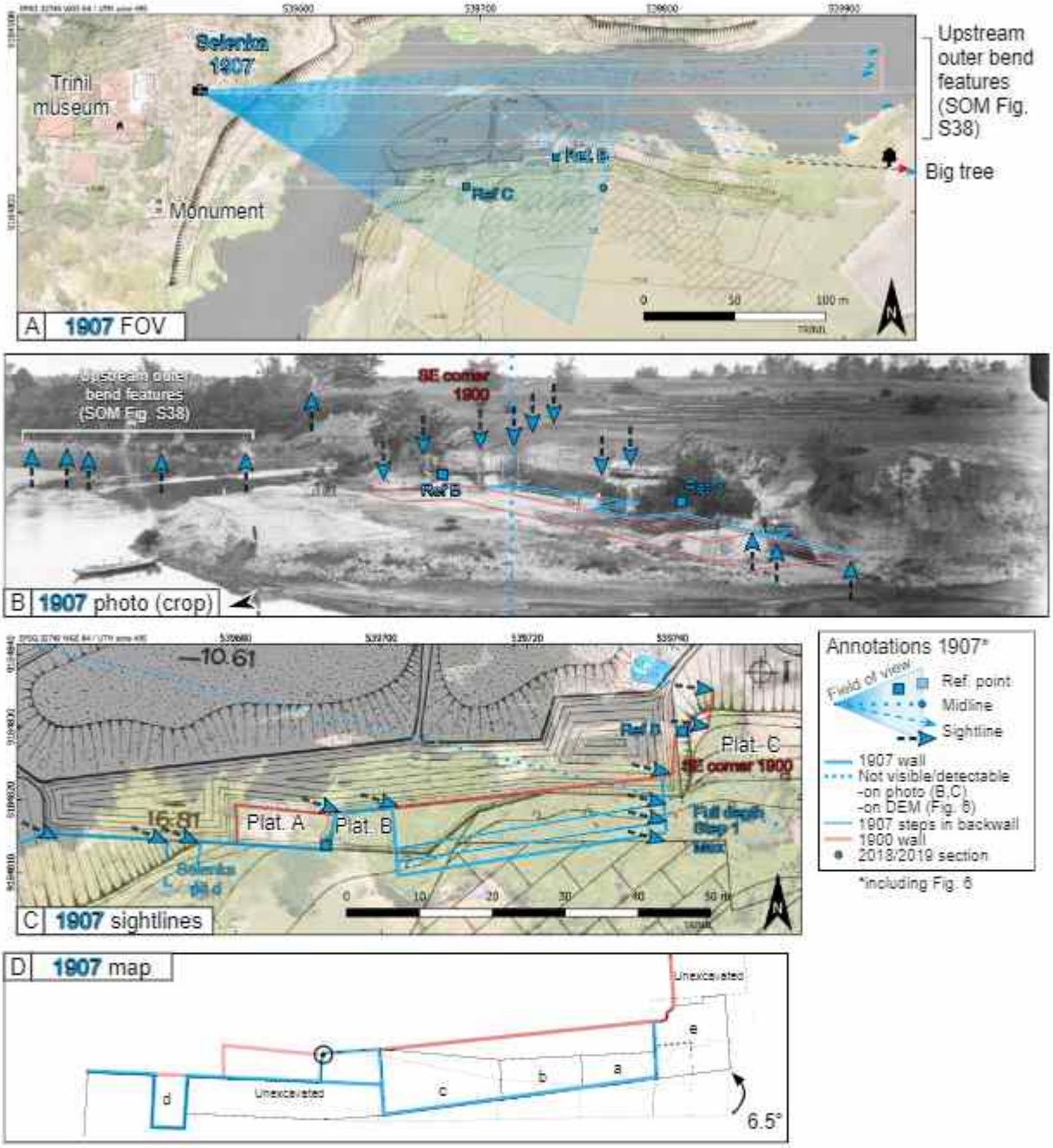

Figure 5. Field of view (FOV) assessment and sightline analysis of the 1907 image; (**A**) Field of view of the 1907 photo shown on the georeferenced 1900 map/drone imagery (for reference); (**B**) cropped 1907 photo with reference points, 1907 (↓ 1900) pit outline, and sightlines (arrows); (**C**) detailed map with reference points, 1907 pit outline, and sightlines; (**D**) 1907 map outline and changes made to fit with the 1900 situation and sightlines obtained for the 1907 photo. Abbreviation: Ref. – reference point; Plat. – platform.

any of the foreground features of the later imagery. Using known background features, including those visible in the upstream outer bend of the Solo River (Fig. 7; SOM Fig. S38) and the Kendeng range in the far background (SOM Fig. S39), the camera position and FOV of the 1894 photo could be determined (Fig. 7A; see SOM S1 for details).

Position of the 1891–1893 excavation pits With the 1891–1893 pits being situated further into the river than those of 1900 and 1907, their position can only be spatially reconstructed by looking at the very low wall remains that can be found there (Fig. 8) and identifying how they intersect with sightlines obtained from the 1894 photo, for which the camera position and FOV was established. In the 1894 photo (Fig. 7B), one of the most characteristic features visible is the southeast corner of the back wall, making a >90° angle. Such a corner (~115°) can be seen on the DEM, situated exactly on the sightline for this feature (arrow 'SE' in Fig. 8). From here the low excavation wall can be followed in a west–southwest direction, which differentiates it from the (close to) east–west oriented low wall remains to the south that can be linked to the 1900/1907 excavations. The change in pit orientation most likely took place in 1899, when, after several years of no or only

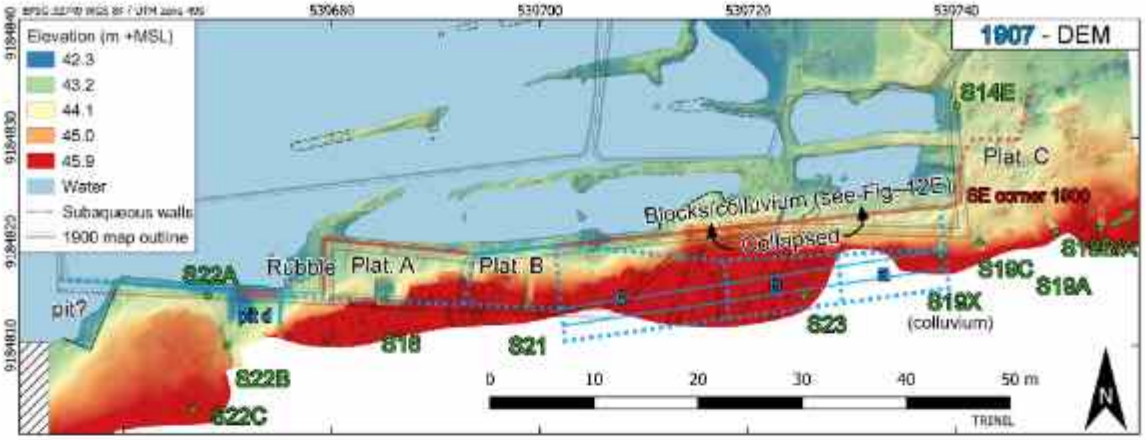

Figure 6. Reconstructing the position of the 1907 pit in relation to the 1900 pit and the remains visible at the present day, shown as a digital elevation model (DEM). Abbreviation: Plat. — platform.

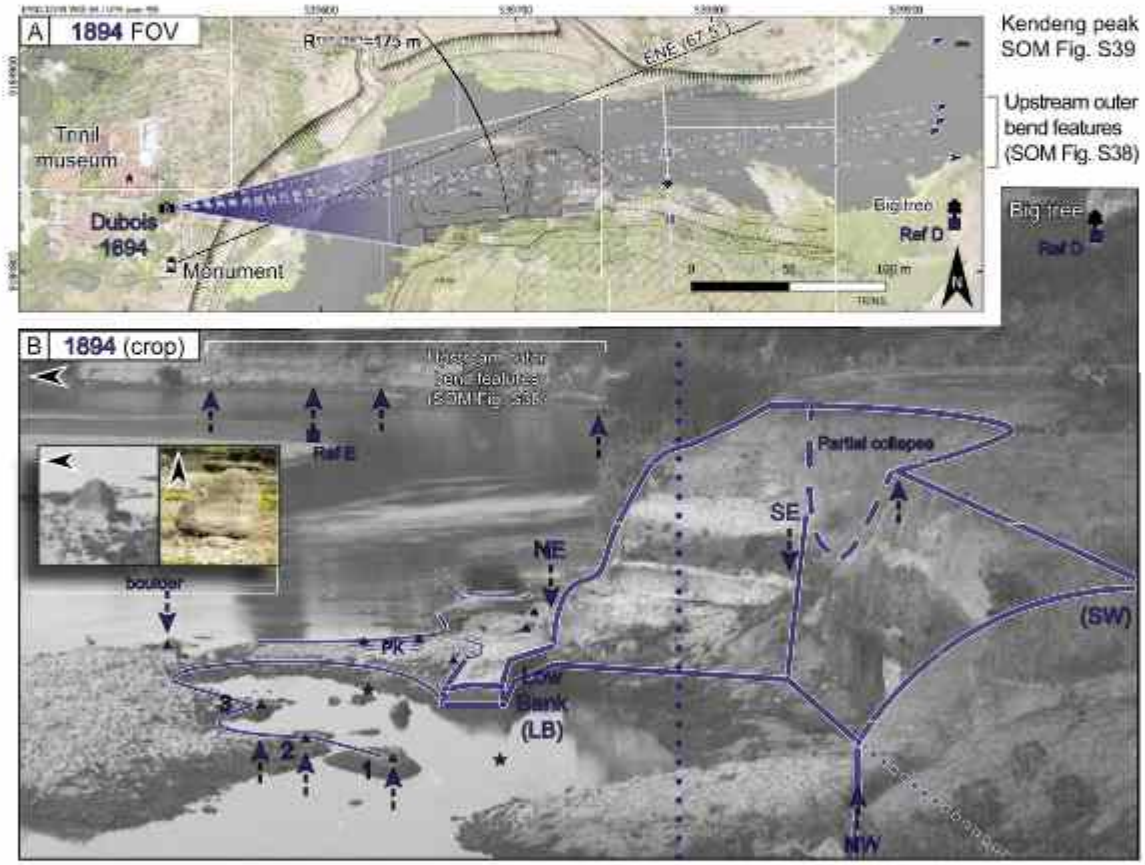

Figure 7. Field of view assessment and sightline analysis of the 1894 image. See Figure 8 for legend. (**A**) Field of view of the 1894 photo shown on the georeferenced 1900 map/drone imagery (for reference) and the '175 ENE' information contained on the Dubois monument indicating the location of the findspot of *Homo erectus* plotted as a black arc and line; (**B**) 1894 photo (cropped) with reference points, pit outline, and sightlines (arrows). Abbreviation: Ref — reference point.

small pits being dug on the left bank, large-scale excavation recommenced along a square meter grid system (SOM Fig. S28A). Noteworthy is also the collapse in the back wall—a recurring feature in the Trinil excavation imagery.

On both the 1894 photo and DEM, the wall continues north by east (~10°) from the southeast corner. This shorter east wall is, due to its orientation facing the camera, particularly suitable for stratigraphic interpretation (see section 3.4). The wall connects near water level to a low, relatively straight-lined low bank (LB) of well-consolidated sediments (middle of Fig. 7B), standing out among the colluvium and spoil material. Sightlines for the LB place it where now a 'negative' of this feature can be found on the DEM (Fig. 8A). This negative follows the outline visible in the photo, including the flaring sides at its eastern end (see SOM Fig. S40 for side-by-side comparison with the present-day 3D model). It appears to have been excavated down to the top of the BGL-5 lahar deposits, which

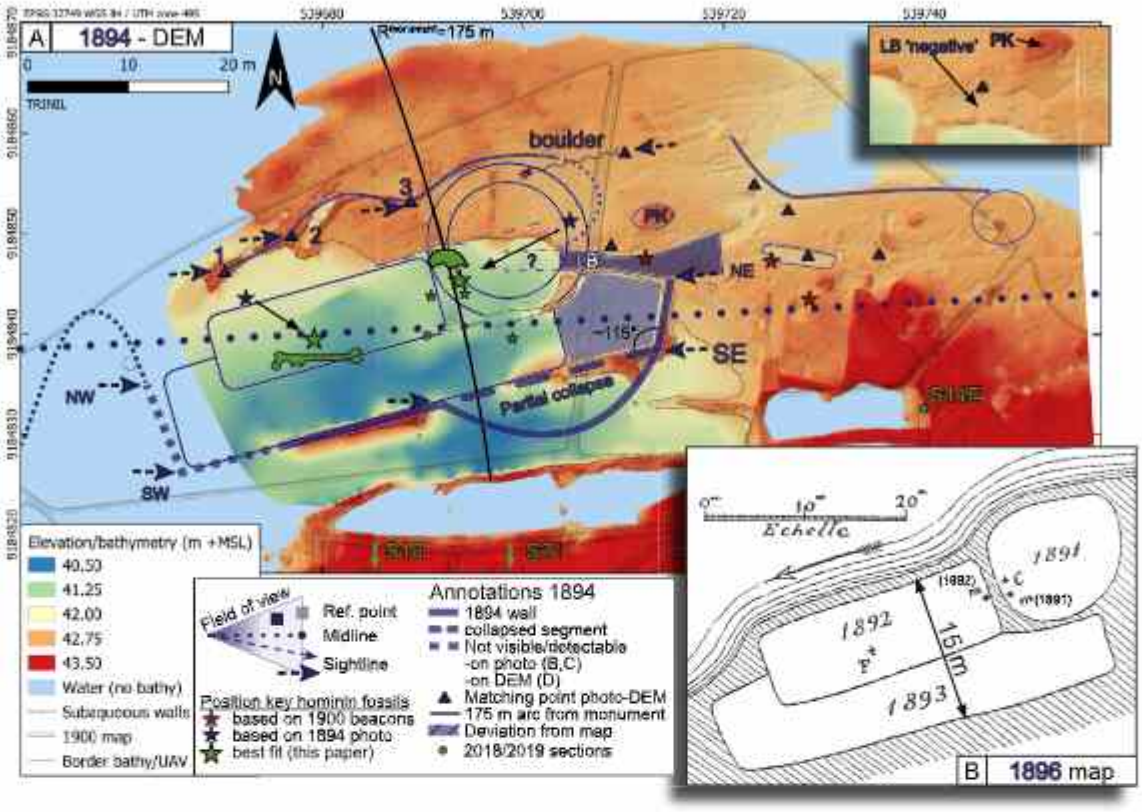

Figure 8. (**A**) Reconstructing the position of the 1891–1893 pits in relation to the remains visible at the present day, shown as a digital elevation model (DEM). Sightlines (see Fig. 7) were required to constrain their position. Note: arrows representing sightlines are on the righthand part of the figure inversed for clarity. (**B**) Map from Dubois 1896 publication showing the 1891–1893 pits. Abbreviations: F – Femur I; m – molar; C – calotte.

only rarely yield fossils (see Hilgen et al., 2023). This feature was most likely described in a field letter as a 6 m^2 ledge that was (independently) excavated after the river level receded (Kriele and de Winter, 1895a). One year later, the remains of this ledge were removed, yielding shells and bones (Kriele and de Winter, 1896); exactly what was recovered in 2018–2019 from the surface of and within a small 20 × 20 cm pit in the 'PK' feature (Fig. 8). This 'Pulau Kerang' (literally 'Shell Island'), situated just 6 m from the LB (Fig. 8A and inset), is an elevated patch of BBC-1 deposits directly overlying BGL-5, yielding numerous fossil *Pseudodon* shells as well as vertebrate fossils.

Additional photo features are harder to distinguish and compare with the DEM due to large amounts of colluvium and spoils and possibly somewhat higher water levels on the photo. The large boulder in the photo is very likely to be the same as the one encountered in the field today (Fig. 7B, inset). However, despite the attempts to include it and its known present-day position in the FOV assessment, it was not possible to integrate the big boulder as well as all other reference and control points. It also seems to be situated further away from the camera position relative to the low bank and southeast wall in the photo, and is, unlike other boulders on the site, not embedded in sediment (Fig. 7B). It, therefore, most likely shifted several meters downstream to its current position (Fig. 8A). The heart-shaped shoreline visible in the photo (Fig. 7B) between the big boulder and the LB does seem to be recognizable on the DEM (Fig. 8), supported by sightlines for several larger features (blue triangles 1–3 in Figs. 7 and 8A).

On the DEM, starting just north of the LB, a pit edge (thin dashed line, Fig. 8A) can be seen running more or less parallel to the 1894 back wall. Together they create an accommodation space of ~15 m wide, which matches the combined width of the 1892 and 1893 pits on the earliest and most detailed map documenting them (Fig. 8B; Dubois, 1895c). At the eastern end, the boundary between the 1892 and 1893 pits can still be distinguished on the DEM by subaqueous wall remains (Fig. 8A). It surfaces as a quadrant connecting to the LB; most likely the southeastern part of the 1891 pit (circle in Fig. 8A). The 1891 pit has been described in letters and represented in (other) maps as apparently having various shapes and dimensions. This can be best explained by the fact that at this location fossil-rich deposits were situated close to the surface (Dubois, 1896a), making it possible to recover them in an ad hoc fashion (i.e., without digging a deep or well-defined pit).

The 1892 pit required more planning as it involved the removal of substantial amounts of overburden (Kriele and de Winter, 1892a; Dubois, 1893b). At its eastern end, it did however cover the southern part of the 1891 pit (Dubois, 1896a) and was excavated 2 m below 'low water level', as later recalled (Kriele and de Winter, 1895b). The 1893 pit was in turn excavated 1 m deeper than that of 1892 (Kriele and de Winter, 1893). Although the continuous process of erosion/deposition by the present-day Solo River makes an absolute comparison difficult, the relative depths mentioned in these letters seem to be reflected in the bathymetry model and the reconstructed positions of the pits presented here (Fig. 8A). The proposed pit positioning leaves an area of ~7 × 8 m east of the 1893 pit (shaded area Fig. 8A), which was either included in the latter or not fully excavated yet and finished as a near-water level extension of the later 1897 pit (that was most likely situated where the partial collapse is visible on Fig. 7B; see SOM Fig. S27).

Position of hominin fossils (Femur I, skullcap, molars) The most precise—but not necessarily accurate—source of information

regarding the find spots of the hominin fossils are the intersection points (red stars in Fig. 8A; see also Fig. 3B, C) of the three 1900 beacons supposedly indicating the position of skullcap, Femur (I), and molar (Kriele and de Winter, 1900a). These positions, however, fully contradict the pit positioning presented above (blue lines) and the distance of 175 m (black arc in Fig. 8A) as indicated on the Dubois monument (SOM Fig. S34B). An alternative positioning of the fossils based on the 1894 photo and derived sightlines for the locations of Femur I and the skullcap indicated by Dubois on an annotated version of the photo (see SOM Fig. S3), and an approximation of their relative distance from known site features (e.g., LB, in the southeast corner), yields the positions indicated by the blue stars (Fig. 8A). Although more compatible with the 1891–1893 pit positioning and distance indicated on the monument, the reconstructed distance of 32 m between the skullcap and Femur I places them too far apart, given the distance of 10–15 m indicated in letters and publications (Dubois, 1894a, 1894b, 1932a, 1934). When Femur I and the skullcap are positioned according to the 1896 map and how that map fits on the DEM (green stars in Fig. 8A), the skullcap sits exactly on the 175 m line from the monument, with Femur I situated 15 m west–southwest of it. Although approximate (i.e., with an error margin of a few meters), these seem to be the best approximations of the find localities of the skullcap and Femur I. The 1891 and 1892 molars were found, respectively, 1 m from the skullcap and ca. 3 m from the skullcap in the direction of Femur I (Dubois, 1896a), as also indicated on the 1896 map (Fig. 8B).

The differences between the positions reconstructed here, those visible on the annotated 1894 photo and those marked by the 1900 beacons, are striking, but not surprising. There is a large distance between the 1894 camera position and the excavation area relative to distances between particular site features. This leads to apparent (visual) depth compression of the image, which, together with large amounts of colluvium and debris on the site (and potentially higher water levels), may have led to Dubois erring in labeling the 1894 photo. It is also worth considering that Femur I was excavated in August 1892 (Dubois, 1893a)—possibly in a test pit-like exposure—before the excavation of the larger 1892 trench commenced (Kriele and de Winter, 1892b, 1892c; Dubois, 1893b; Joordens et al., 2015). When it comes to the beacons, uncertainty regarding the position of the fossils and the pits they were found in was expressed in the excavation letters and attributed to the 4–5 m of spoil overburden and the removal of as many low walls ('dijkjes', in Dutch) as possible (Kriele and de Winter, 1900b). Although attempts were supposedly made to uncover and find the 1891–1892 pits (Kriele and de Winter, 1900b), no further mention was made of this initiative in the letters and the position of the beacons shows that they were clearly unsuccessful.

3.4. Stratigraphic analysis: Eastern part

Here the stratigraphy of the eastern part of the historical excavation area is assessed (as visible in 1900 and 1907 imagery) and compared with 2018–2019 sections S18, S19, and S22.

Historical imagery 1900/1907 Due to its orientation, vertical coverage, and unobstructed view, the 1900 east wall on photo 1900-II documents the stratigraphy at the eastern end of the excavations very clearly (Fig. 9A). The same wall is also visible in 1907, as well as the southward extension made that year (Fig. 9B). Unit 1 in the 1900 photo is fairly dark, which may be due to increased water saturation near water level. Unit 2 is lighter-colored and appears relatively coarse with horizontal bedding. Above unit 2, a darker-colored and seemingly finer-grained layer is visible with no apparent structure (unit 3), but it seems to consist of less-consolidated material, creating a slight overhang of the overlying, more consolidated white layer (unit 4). After an irregular contact follows a dark-colored layer, most likely silt or clay (unit 5). The overlying layer (unit 6) shows quite some variability in color, which could be related to variable degrees of water saturation (i.e., the wall drying out due to prolonged exposure). However, the interbedding of darker and lighter layers is visible in the southeast corner of the 1907 photo (Fig. 9B), which can also be seen on the short south wall (SOM Fig. S11). The color difference between the lower and upper parts of unit 6 on the south wall is not visible on the east wall. Unit 7 is difficult to assess as it is largely affected by collapse (see also far left in Fig. 14A). The contact with unit 6 is clearly visible on the south wall but can be distinguished on the east wall as well. The succession continues on the south wall with unit 8, which can be identified as a conglomerate (Fig. 12C). This is overlain by finer-grained deposits up to the vegetation of the sawah. The 1900 southeast corner shows a collapse reaching up to the base of unit 7 (Fig. 9A–B). In the 1907 photo, the surface of platform C was worked to a lower level rendering the same collapse difficult to discern, but further south a small channel incision cutting down to the base of unit 7 can be seen.

2018–2019 stratigraphy Although most of platform C has been removed in 1908, the 2018–2019 sections dug in the present-day river bank just to the south of it each yielded primary deposits (Fig. 9C–D). Of the historic east wall (red line in Fig. 9), only the lowest part has been preserved, including Section S14E in the northern half. From the southeast corner, the wall runs west behind secondary blocks originating from a higher stratigraphic position (see sections 3.2 and 3.5). South of that lies the 1907 pit (cyan line); a test section dug there (S19X) yielded (as expected) only colluvium. The low-lying (<44 m +MSL) outcrops north of the present-day river bank—as visible on the DEM (Fig. 10)—can in most cases be connected to the stratigraphy visible in the eastern sections.

The stratigraphy encountered at the east end is summarized in the composite stratigraphic column (Fig. 9E; see Hilgen et al., 2023, for detailed descriptions). Overlying a clay (Batu Gajah Clay 2 [BGC-2] sensu Berghuis et al., 2021) that is only visible in outcrop at the northeastern corner of the site (Fig. 10) lies a poorly sorted, matrix-supported, volcanic breccia (Batu Gajah lahar 5 [BGL-5] sensu Berghuis et al., 2021). This unit is extensively exposed in outcrops further north (Fig. 10). This is followed after an unconformable contact by a poorly sorted, sandy-silty, matrix-supported, fossil-rich conglomerate rich in volcanic clasts, interspersed with silt layers, interpreted as a fluvially reworked BGL-5 lahar (Berghuis et al., 2021) that is referred to as Bone-Bearing Channel 1 or BBC-1 (sensu Hilgen et al., 2023). After another unconformity, this is followed by a ca. 2 m thick, planar cross-bedded, moderately sorted, fossil-rich, sandy conglomerate with occasional lenses of finer sediments (sand or silt) that is referred to as Bone-Bearing Channel 2 or BBC-2 (sensu Hilgen et al., 2023), that largely cuts through the BBC-1. The BBC-2 is very rich in reworked soil concretions, most notably toward the top. Although not very well-sorted, the cross-bedded structure seems to indicate that it is a fluvial deposit. Although largely removed by the historical excavations, remains of BBC-1 and BBC-2 deposits are still visible in outcrops north of the present-day riverbank (Fig. 10), in which test pits were dug (see below). The sections and outcrops indicate a southeast–northwest orientation for both the BBC-1 and BBC-2 channels, with their infills wedging out against the BGL-5 lahar toward the northeast (Figs. 9C–D and 10).

The BBC-2 layer is unconformably overlain by ca. 80 cm of cross-bedded sands and silts, which did not yield fossils and was less consolidated compared to the underlying deposits. Toward the top, it is indurated into a hard, white bank. This seems to be the result of diagenesis as the induration intersects cross-bedding structures. On the irregular unconformable contact lies a massive grey-brown to dark grey clayey-silt/silty clay, of which the lower part is rich in

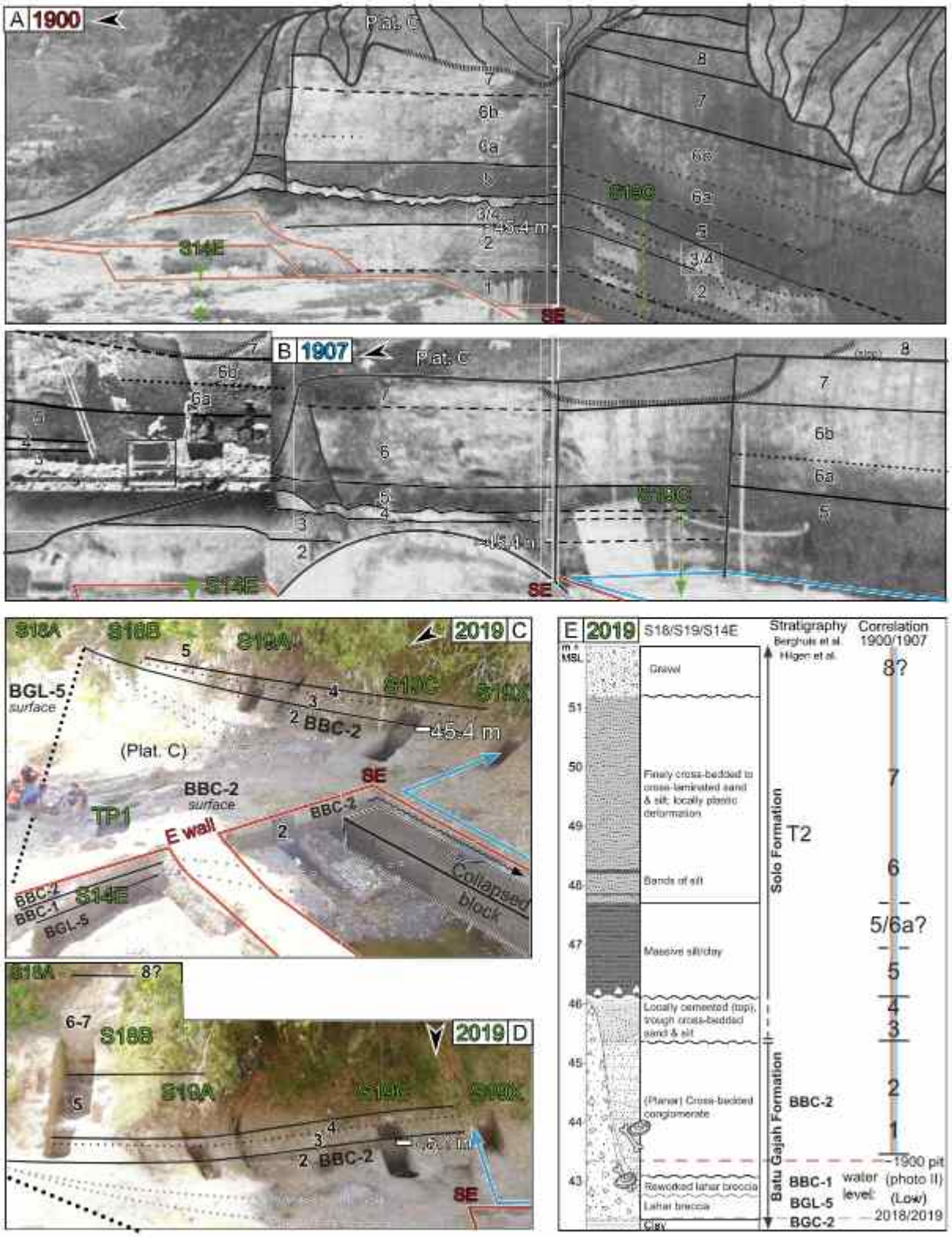

Figure 9. Stratigraphy of east end 1900/1907 excavations compared with 2018–2019 stratigraphy. (**A**) stratigraphy visible on the east (and parts of) the south wall on 1900 photo II; (**B**) stratigraphy visible on the (extended) east wall and (parts of the) south wall of the 1907 photo; the inset shows the track running at approximately the top of unit 2; (**C**), (**D**) eastern part of historical excavations in 2019 with exposed sections (see Hilgen et al., 2023 for detailed imagery); (**E**) composite stratigraphy of S18B, S19 and S14 and correlation with historical stratigraphy (see Hilgen et al., 2023 for individual section drawings/photographs and their correlations). Scale bars have an interval in meters, (approximate) absolute elevations are indicated in meters above mean sea level. Abbreviation: Plat. = platform.

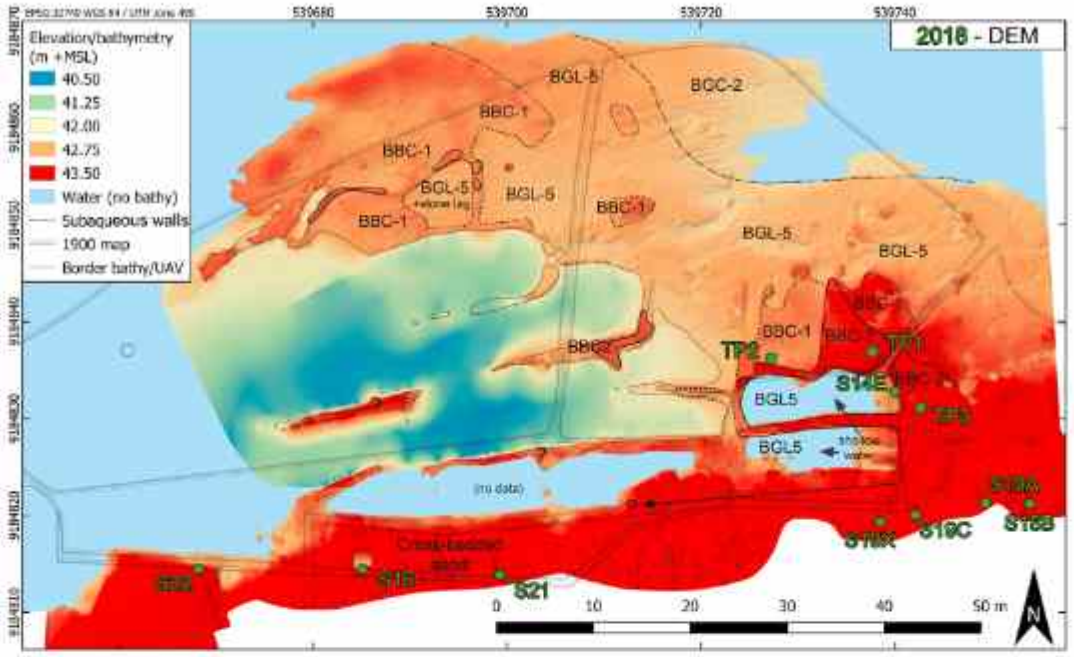

Figure 10. Digital elevation model (DEM) of the historical excavation area and the annotations indicating the stratigraphic units exposed at the surface (see Fig. 9E for reference). The location of the test pits (including TP1; see Fig. 11) and sections are indicated for reference.

plant remains. Following (but only exposed in S18B) is a thick layer of well-consolidated (cross-) laminated (fine) sand and silts, which is brown-grey in the lower part and increasingly light grey-yellow toward the top. In the lower part, bands/lenses of finer material are visible. This succession is after an unconformity capped by unconsolidated brown-grey gravel. The deposits overlying the BBC-2 are interpreted as fluvial deposits that belong to the T2 terrace of the Solo Formation (sensu Berghuis et al., 2021; see also Hilgen et al., 2023).

Correlation The proximity of the 2018–2019 sections to the historic east wall and the clear stratigraphic similarities between them, allowed for a relatively straightforward correlation (Fig. 9E), particularly for units 2–5. Based on absolute elevations (calibrated on the interface between units 2 and 3), both units 1 and 2 correlate with the BBC-2, with unit 1 being darker due to water saturation. The BBC-1 is thus sitting below water level in the 1900 photo. The looser, cross-bedded sand/silt above the BBC-2 and the indurated bank above that can be directly correlated with units 3 and 4 in the historical imagery. Units 5–8 could only be exposed in Section S18B, which is situated further to the east, making correlation with the more westerly lying 1900/1907 walls more tentative (i.e., due to possible lateral variation). Nevertheless, the presence of first (dark-colored) massive silt/clay and (lighter-colored) finely structured sand/silts are clearly recognizable in the historical imagery as units 5 and 6/7. In both S18B (gravel) and the historical imagery (unit 8 conglomerate), a coarse layer is visible in the top part of the section, but given the difference in consolidation, the difference in vertical position (+1.5 m in S18B), and distance between the two locations, their correlation remains tentative.

Test pits and the identification of the primary targets of the historical excavations The excavation of three test pits (TP1–3, Fig. 10) revealed that the two units exposed in them, identifiable as the BBC-1 and BBC-2 (see also Hilgen et al., 2023), are both highly fossiliferous—together yielding 458 fossils from 1.7 m^3 sediment. Of these, 356 were measured by DGPS. The deepest pit, TP1 (Fig. 11), yielded the largest number of fossil finds ($n = 203$; DGPS measured finds from 0.8 m^3) of which most were found in the BBC-2 deposits ($n = 156$). The BBC-1, separated from the BBC-2 by a lens of silt that sits at the top of the BBC-1, was notably less fossil-rich ($n = 47$). The BBC-1 and BBC-2 in the test pits (see also SOM Fig. S41) contain vertebrate fossils, fossil bivalve mollusks, and plant/wood remains, but the BBC-1 seems proportionally richer in bivalves and (large) wood remains (e.g., branches in TP2 and tree trunks found in BBC-1 outcrops between TP1 and TP2, see Hilgen et al., 2023; SOM Fig. S4A). The sections and outcrops show that the underlying BGL-5 and overlying cross-bedded sands/silts are relatively poor in fossils.

The stratigraphic position, lithology, and fossil content of the BBC-1 and BBC-2 largely agree with the historical descriptions and figures by Dubois, Oppenoorth, Carthaus, and Dozy of the fossiliferous deposits excavated near low water level. Dubois described

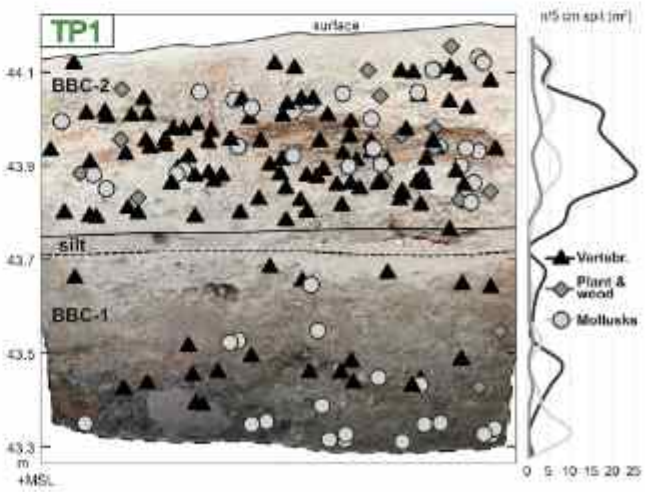

Figure 11. Vertical distribution of fossil finds from the 1 m^2-sized TP1, which covers deposits of BBC-1 (including silt layer) and BBC-2. See SOM Figure S41 for the vertical distributions of the other two test pits (TP2, TP3).

two fossiliferous units yielding vertebrate fauna, freshwater shells, and even tree trunks (Dubois, 1892a): a highly fossiliferous lapilli layer, and below that, a conglomerate that contains few bones, whereas the black clay below that yielded none (Dubois, 1896a). The BGC-2 clay is in the 2018–2019 stratigraphy underlying the BGL-5 lahar (Fig. 9E), but the latter thins toward the west and the BGC-2 is, therefore, likely to underlie the BBC-1 where Dubois dug his 1891–1893 pits. Similarly, the apparent lower find density in Dubois' conglomerate than that of the BBC-1 may be based on observations made further west at the site and the result of variable levels of reworking of the BGL-5. Oppenoorth describes a basal fossiliferous part of the H.K. level as being coarser with large volcanic clasts, as opposed to its finer middle and upper parts that contain 'hard clay nodules' (Oppenoorth, 1911)—possibly referring to the soil nodules that particularly accumulate at the top of the BBC-2. Carthaus also recognized one 'Knochenschicht', consisting of lapilli to boulder-sized volcanic material and yielding vertebrate fossils, shells (including *Unio*, i.e., *Pseudodon*), tree trunks, and branches (Carthaus, 1911a). Interestingly, Dozy distinguished on the right bank a fossiliferous conglomerate ('Harter Konglomerattuff') between the 'Konglomerattuff' and the H.K. (Dozy, 1909, 1911a), particularly in two sections (Dozy, 1911a: Plate X) that intersect that of Carthaus (who only distinguished one find-rich level). In one section (B), the fossiliferous conglomerate and H.K. are toward the south separated by a clay layer, which may have contributed to their recognition as separate strata on the right bank.

That the top of the H.K. corresponds to the top of unit 2/BBC-2 is supported by Dozy's accurate description of the deposits overlying the H.K. at the left-bank excavation (Dozy, 1909: 609), matching those observed in the historical imagery and in the 2018–2019 sections. Furthermore, according to Oppenoorth (1911), both the H.K. and the Decauville track were situated at the same level below the fossil *Stegodon* remains found in unit 7 when he oversaw the work in June/July of 1907. Imagery from that period indeed shows the track sitting at the same elevation as unit 2 (Fig. 9B inset, SOM Figs. S13–S14; note: the track was situated lower in August, i.e., Fig. 9B).

3.5. *Stratigraphic analysis: Middle part*

Here the stratigraphy of the central part of the historical excavation area is assessed (as visible in the 1900, 1907, and 1894 imagery).

Historical imagery 1900/1907 In the 1900 photo, the series of units 1–8 can be followed for some distance along the south wall (Fig. 12A, C). The lower resolution 1907 photo (Fig. 12D) reveals fewer details, aggravated by a more or less uniform, dark (water-saturated?) appearance of the lower part. Accessory 1907 images (SOM Figs. S13–S14) are of better resolution, but there the wall shows various levels of progress/cleaning, and the Decauville track and its foundation obscure the view on the lower part of the stratigraphy, including the fossil-bearing levels. In the 1900 photo (Fig. 12A, C), units 1/2 show lenses, which are partly weathered out of the wall producing characteristic undercuts. The undulating (diagenetic) hard bank observed in the east wall (unit 4) is recognizable, but appears more irregular here and situated lower in the cross-bedded sands. Toward the west, units 2–4 are interrupted by a channel cut, which deepens toward the west where the group of workers is excavating in the 1900 photo (Fig. 12A; see also Fig. 12C). The exact depth and the number of fills of this channel cut are difficult to establish based on the imagery. A finer-grained fill is clearly visible reaching close to the water level in the pit, while the wall surface below that could either represent a coarser lower fill or (BBC-2) deposits affected by surface exposure (i.e., mud drapes, drying). Evidence for a deep incision is however provided by 2018–2019 section S16 (see below), which shows an absence of BBC-2 and BBC-1 deposits well below water level. The fine-grained deposits of unit 5 are clearly visible, but the contact with overlying unit 6 appears gradual (Fig. 12A, C). The lower part of unit 6 (a) is darker/finer-grained, while the upper part (b) is generally lighter colored (Fig. 12; SOM Figs. S6–S7, S13–S14). Beds of alternating lighter/coarser and darker/finer sediments are visible, but are, contrary to the 1907 east wall, inclined (SOM Fig. S7). Unit 7 follows after a clear contact, showing variation in color that can be partly attributed to exposure (i.e., vertical dark bands). Accessory 1907 imagery (SOM Figs. S13–S14) reveals plastic deformation between a lighter-colored top part and a darker bottom part. The fossil *Stegodon* and *Hippopotamus* remains situated in this layer (Fig. 12D; SOM Fig. S15) were indeed said to have been recovered from a light grey clay (Oppenoorth, 1911). Unit 8 is visible in the 1900 photo but cut off on both sides by collapses (Fig. 12A, C). Unit 8 is also visible in the 1907 imagery (Fig. 12D; SOM Figs. S13–S14), but here flanked by clearly visible channel cuts that are probably small-scale erosion gullies. Given their positions, it is reasonable to assume that the 1900 collapses took place where these gullies—filled with younger, less consolidated sediments (Oppenoorth, 1911)—were exposed in the back wall. The total stratigraphic succession, visible in the 1900 south wall, measures ~9 m from water level to the top of the section.

Historical imagery 1894 Using the reconstructed location of the 1891–1893 pits (Fig. 8A), elements of these pits can be (approximately) projected in the 1900 imagery (Fig. 12A–B). The 1894 east wall provides the best view of the stratigraphy exposed during the 1891–1893 excavation and shows a very similar succession as is visible on the 1900/1907 east wall and large parts of the south wall. The strata appear to be inclined, but this is most likely due to the oblique viewing angle on both the horizontal (Fig. 8A) and vertical axes (i.e., high camera position; SOM Fig. S30B). The basal succession of units 1–4 is clearly visible. Therefore, the lower channel cut identified in the 1900 back wall must have missed the 1894 east wall and ran west of it (orange arrow Fig. 12A–B) in a southeast–northwest orientation. Due to a very oblique viewing angle on the 1894 south wall (not shown completely here, but see Fig. 7B), it is not very well visible, exacerbated by a large collapse at its eastern end. Given the depth and spatial position of the collapse, it is most likely an extension of the erosion gully identified in the 1900/1907 photos. Unfortunately, the colluvium from this collapse obscures the view of the lower stratigraphy, including the expected lower channel identified in the 1900 photo.

Correlation with 2018–2019 stratigraphy During the 2018–2019 fieldwork, it was not possible to document large sections along the 37 m long main Selenka pit: its back wall is situated at least 8 m south of that of the 1900 pit (Fig. 12D–E; see plan view in Fig. 6) and in front of it lies a substantial amount of colluvium. However, the border between the 1900 and 1907 pits is still visible as a low wall, consisting of BBC-2 deposits (Fig. 12E). In front of this wall and inside the 1900 pit, large blocks of sediments were found in secondary position. The lower part of the blocks consists of clayey silt (or silty clay) with a frequent occurrence of freshwater snails and the upper part consists of fine cross-bedded/laminated sand. At the eastern end, the blocks appear to be lying horizontally, but at the western end, they are in an angled position. The same blocks, albeit in a more complete state, are documented by early, accessory 1907 imagery (SOM Figs. S10–S12), revealing a stratigraphy that can be correlated with units 5/6–8. Later, the area where the blocks were situated was leveled at or just above the top of BBC-2 to lay the Decauville track (Oppenoorth, 1911; SOM Figs. S13 and S14), which necessitated the removal of the uppermost parts of the blocks. Their lower remnants, covering units 5/6 and still carrying characteristic tool marks, survived up to the present-day, as they are situated below the top of the BBC-2.

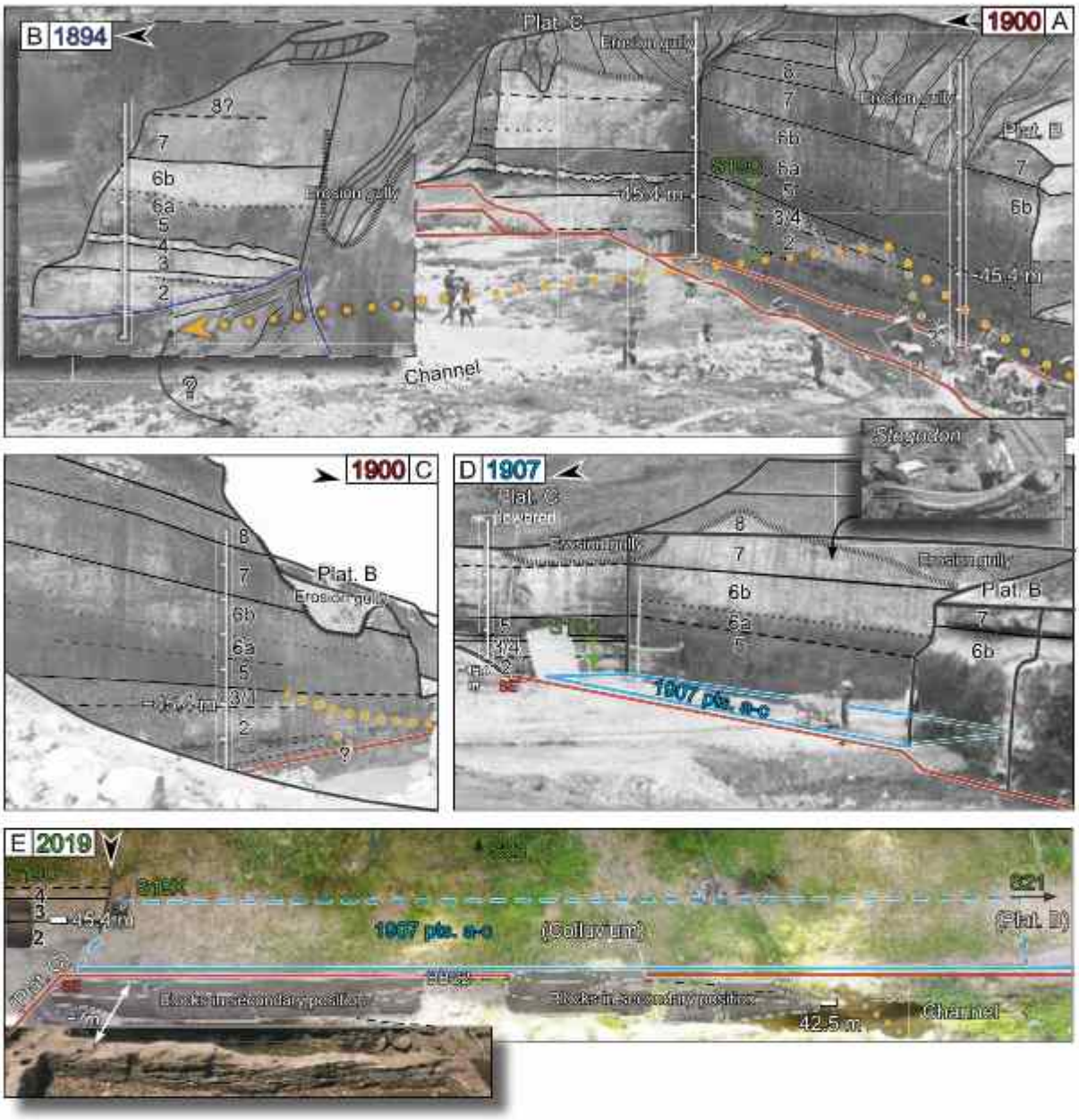

Figure 12. Stratigraphy between platform C and B of the 1900/1907 excavations compared with the 2018–2019 situation (which did not yield long sections of primary deposits). Stratigraphy visible on the east and south wall of 1900 photo II (**A**) and the east wall of the 1894 photo (**B**), whose approximate position relative to the 1900 photo could be established using the sightline analysis; (**C**) same wall as in A, but seen from the camera position of photo I (see Fig. 3A); (**D**) stratigraphy visible on the east wall and south wall on the 1907 photo; the inset shows the Decauville track at approximately the level of the top of unit 2; (**E**) oblique orthophoto of the area between platform C and B in 2019; the inset shows the east–west running wall running parallel to the 1900 back wall, but here unobstructed by secondary deposits and revealing planar cross-bedding and (partly undercut) lenses. Scale bars have an interval in meters, (approximate) absolute elevations are indicated in meters above mean sea level. Abbreviation: Plat. = platform.

A better exposed, unobstructed 16 m long low wall of BBC-2 deposits can be found running parallel to the 1900 back wall, about 7 m north of it, dividing the easternmost part of the 1900 pit in a northern and southern half (Fig. 12E; see also Fig. 4.) This low wall shows planar (cross-) bedding. Notable is the differential erosion of the finer (silty) interbeds, creating lens-shaped undercuts/overhangs within and at the base of the BBC-2 deposits, similar to what is visible in the 1900 back wall (Fig. 12A, C).

Within the 1907 main excavation area (blue area in Fig. 12E), remaining primary deposits could only be found at a very short section (S23) higher up in the river bank (48.5 +MSL). This short section is situated where the wall of the first step of the 1907 excavation is expected to be (Fig. 6) and documents cross-laminated sands and silts similar to those observed at the same level in S18B (see composite stratigraphy in Fig. 9E) and in the top of S21 (see below).

3.6. Stratigraphic analysis: Western part

Here the stratigraphy of the western part of the historical excavation area is assessed (as visible in the 1900 and 1907) and compared with 2018–2019 Sections S21, S16, and S22.

Historical imagery 1900/1907 At platforms A and B in the 1900 photo, the basal part of the stratigraphy is formed by the infill of the

channel (Fig. 13A). Units 5–6 are recognizable on the back wall at platform B as a gradient of increasingly lighter (coarser?) deposits. Around platform A, the unequal light conditions and shorter exposures impair the visibility of the stratigraphy there. Toward the top of unit 6B, the sediments seem to have been eroding from the section creating an undercut below the overhang of well-consolidated deposits of unit 7. This contact can be followed to the south wall of platform A but is cut short by a complex of channel incisions that reach down to at least water level. These incisions also seem to cut through the aforementioned lower channel (and its original western margin area). In the 1907 photo, both the lower and upper parts of the stratigraphy at platforms A and B are not visible due to respective backfill and being covered in vegetation. Only the contact between units 6 and 7 can be clearly distinguished. Just west of (backfill-covered) platform A in the 1907 photo, above pit d, the semi-circular outline of a wall collapse seems to be visible (also visible before excavations started that year; SOM Fig. S8)—right where the channel incisions are visible in the 1900 photo. To the west of that, cross-bedded sediments (of even younger age) can be seen (Fig. 13B). From there, the Trinil

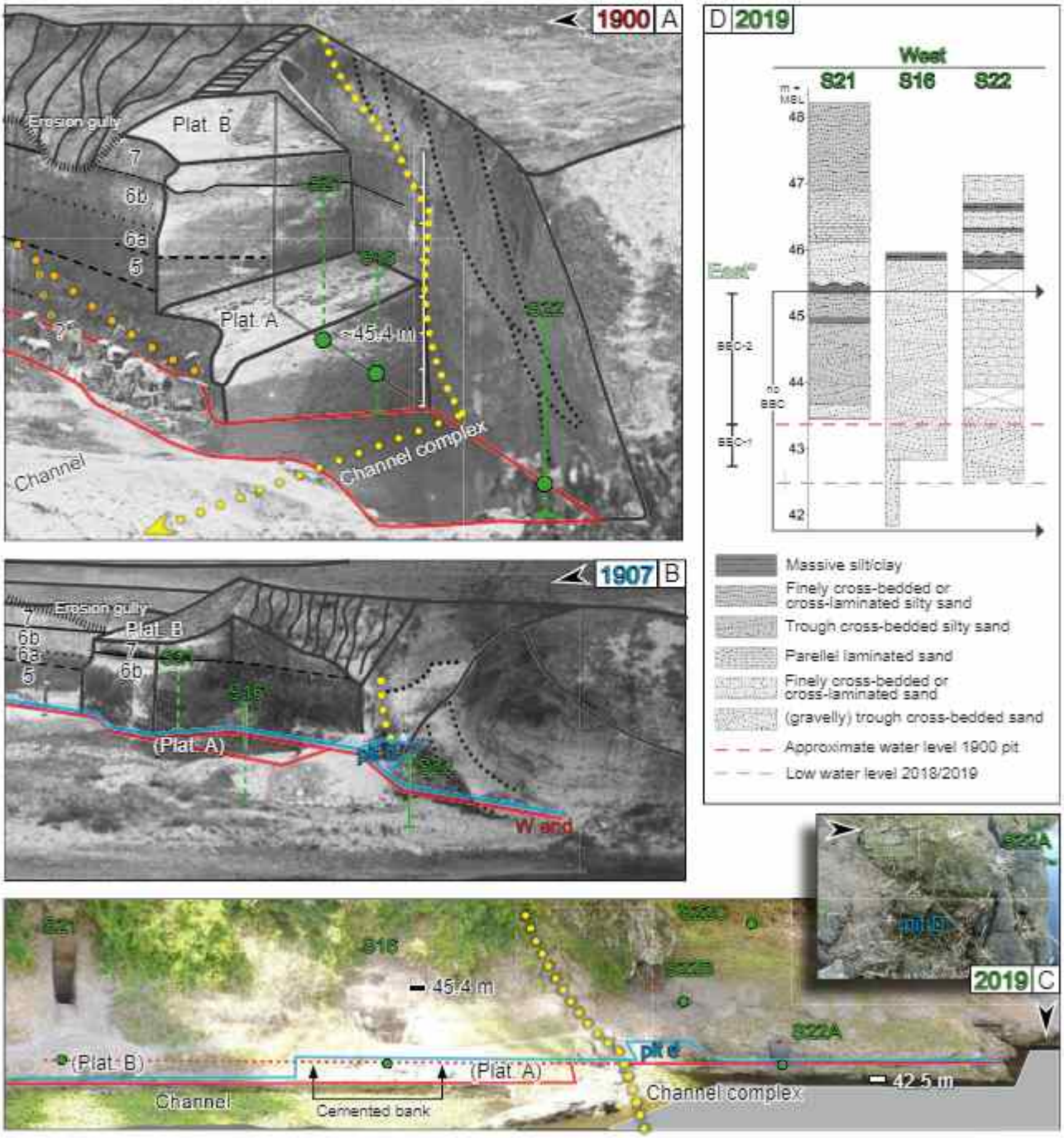

Figure 13. Stratigraphy between platform B and west end of the 1900/1907 excavations compared with the 2018–2019 situation. (**A**) stratigraphy visible on south wall of 1900 photo B; (**B**) stratigraphy visible on the south wall of the 1907 photo; (**C**) oblique orthophoto of the area between platform B and the west end in 2019, with (inset) detail photo of Selenka's pit d; (**D**) 2018–2019 sections documented between platform B and the west end of the historical excavations (see Hilgen et al., 2023 for detailed imagery of the sections). Scale bars have an interval in meters, (approximate) absolute elevations are indicated in meters above mean sea level. Abbreviation: Plat. = platform.

inner bend headland descends toward the present-day Solo River, ending the exposure.

Correlation with 2018–2019 stratigraphy After a large gap of more than 40 m, longer sections could again be exposed at S21 and S16 (Fig. 13C–D). They are situated behind, respectively, platform B and A, in line with (the wall running in front of) S22A further to the west (Fig. 13A–C; see plan view in Fig. 4). Where the eastern sections yielded fossil-rich BBC-1 and BBC-2 deposits, they are absent in sections S21 and S16, despite being dug as deep as or deeper than S19C (Fig. 13D). Rather, at similar levels, these sections show predominantly well-sorted, trough cross-bedded sands and are comparatively poor in (vertebrate) fossils. A notable exception is the find of two well-preserved and articulated fossil bovid vertebrae at 43.4 m +MSL in S16. Toward the bottom of S16, the cross-bedded sands are cemented, which can also be seen in outcrop along the waterline in front of S16 (Fig. 13C). At S16, coring up to 2 m below the cemented bottom of the section yielded similar sandy deposits and a gravel lag that consists predominantly of well-rounded andesite gravel, suggesting long-distance bedload transport in a major river. This contrast with the badly sorted BBC-1/2 deposits with a gravel lag dominated by soil nodules, suggesting more local streams. Based on their fluvial character and position (Fig. 13A), the lower parts of S21 and S16 (<45.5 m) represent the infill of the lower channel identified in the historical imagery and suggest that it reached substantially deeper than the water level indicated on the 1900 photo. The middle and upper parts of S21 are sitting at the same heights as units 5 and 6a in the east and show on the top of a layer of relatively coarse, cross-bedded sands, smaller-scale cross-bedding, or cross-lamination with occasional (massive) silt lenses and an overall fining of sediments (i.e., increased silt component). This indicates lower-energy fluvial deposition. Based on elevation and composition, the deposits exposed in S16 and S21 can be identified as the T2 terrace stage of the Solo Formation (sensu Berghuis et al., 2021).

The first incision of a larger channel complex visible in the 1900 photo (Fig. 13A) and collapse in the 1907 photo (Fig. 13B) seems still recognizable in 2019 as a recess in the river bank (Fig. 13C), sitting just west of former platform A and above Selenka pit d (Fig. 13C inset). To the west, a seemingly reduced (compared to 1900/1907) but still protruding stack of cross-bedded sands and silts (Fig. 13C) can be found, which was documented by sections S22A–C (presented as a composite in Fig. 13D). Given their position within the channel complex, these deposits are younger than those observed in S16 and S21 and generally document low-energy fluviatile deposition.

4. Discussion

4.1. Stratigraphy: Intermittent fluvial incision and aggradation

One characteristic feature of the complex stratigraphy of the Trinil excavation site (Fig. 14) is intermittent fluvial incision and aggradation, which had a strong impact on the genesis, preservation, and composition of the fossil-bearing deposits. At the (left-bank part of the) Trinil site, the BGL-5 lahar (dated at 830–773 ka: Hilgen et al., 2023)—and probably the BGC-2 clay below that—is incised by the BBC-1 (Fig. 14A). The BBC-1 channel infill is not visible in the historical imagery due to higher water levels but could be documented during the new fieldwork and was also dated at 830–773 ka (Hilgen et al., 2023). Well-visible in the historical imagery (units 1–2 in Figs. 9,12) is the BBC-2, which largely cuts through the BBC-1 (Fig. 14A–B) and is filled with deposits of a substantially younger age, at 560–380 ka (Hilgen et al., 2023). Both fossil-bearing channel infills belong to the Batu Gajah Formation (Hilgen et al., 2023), which is part of the pre-terrace stratigraphy (Berghuis et al., 2021). Based on sections (Figs. 9, 12, and 13) and exposures (Fig. 10) at the left bank excavation area, a southeast–northwest orientation could be reconstructed for both channels, wedging out against the BGL-5 lahar in the northeast (purple dotted line; Fig. 14B–C). This wedging out of fossil-bearing deposits was also observed at the same location by Dozy in the easternmost pit (–platform C) of the 1908 excavations (Dozy, 1911b). When the orientation of the channels on the left bank is extrapolated toward the right bank, they intersect with the area covered by the historical right-bank excavations (Fig. 14D). Here, Dubois and Selenka targeted, according to their accounts, the same fossil-bearing layers as they exposed on the left bank, supporting the reconstructed course presented here. The top of these deposits was measured by 'nivellierung'/'waterpassing' (leveling, i.e., using a theodolite) to run more or less horizontally between the excavations on both banks of the Solo River (Dozy, 1909, 1911b).

This was, however, neither the only nor the last time the Trinil site was affected by channel incision. Careful inspection of the historical imagery revealed the presence of a channel cutting through the lower part (units 2–4) of the historical stratigraphy about halfway along the 1900 back wall (Fig. 14A–B). This includes the highly fossiliferous BBC-2 deposits and possibly the BBC-1 as well. This observation agrees with results from the 2018–2019 fieldwork that documented BBC-1 and BBC-2 deposits between 42.5 and 45.4 m +MSL in the test pits and eastern sections, but not at similar elevations in the sections situated at west of the incision (Fig. 14A–C; see also Hilgen et al., 2023). Unfortunately, samples taken from one of these western sections (S16, at 43.4 m +MSL) did not yield definitive ages, with an age range from the late Middle to Late Pleistocene (Hilgen et al., 2023). These deposits can, however, be identified as being part of the T2 terrace that yielded an age of 95 (+56/–36) ka at nearby Grinseng (Berghuis et al., 2021), i.e., terminal Middle to Late Pleistocene. Moreover, the T2 terrace can be correlated with the Ngandong terrace in the Kendeng area (Berghuis et al., 2021) dating between 140 and 92 ka (Rizal et al., 2020). The reconstructed position and stratigraphy of the 1894 east wall (see Fig. 12A–B), showing BBC-2 deposits, indicate that the T2 channel must have incised west of it, i.e., running southeast–northwest (dotted orange arrow with error margin in Fig. 14C). This approximate orientation is corroborated by the discovery of deposits in Section S17 (right-bank) with a similar lithology and luminescence signal as those in S21 and S16 (Hilgen et al., 2023) at depths of up to 44.7 m +MSL. This section lies just south of where most of the Selenka excavations took place (Fig. 14D)—the position of the Dubois excavations there is approximate. The change in lithology is in agreement with corings performed there during the Selenka campaign (Dozy, 1911a). Contrary to the north, east, and west, where the H.K. wedges out (Dozy, 1909, 1911b, 1911a: Plate X), this is not observed to the south where the corings indicate the absence of H.K. deposits. The available evidence, therefore, suggests that the T2 channel had a southeast–northwest orientation, i.e., similar to the older BBC-1 and BBC-2 channels (Fig. 14D). The BBC-1 and BBC-2 deposits can thus be summarized as constituting a narrow strip of highly fossiliferous deposits, which on the northeast side wedges out against the fossil-poor BGL-5 lahar and are on the southwestern side incised by the T2 channel.

Difficult to see during the recent fieldwork, but very obvious from the historical imagery, is the complex of younger channels cutting through the complete stratigraphy (Fig. 14A–B) at the western side of the historical excavation area. These are either related to a younger T2 terrace or—based on superposition—to the T1 terrace (both part of the Solo Formation sensu Berghuis et al., 2021), but both options require testing by absolute dating of these deposits. The steep incision angle of this channel, as visible in

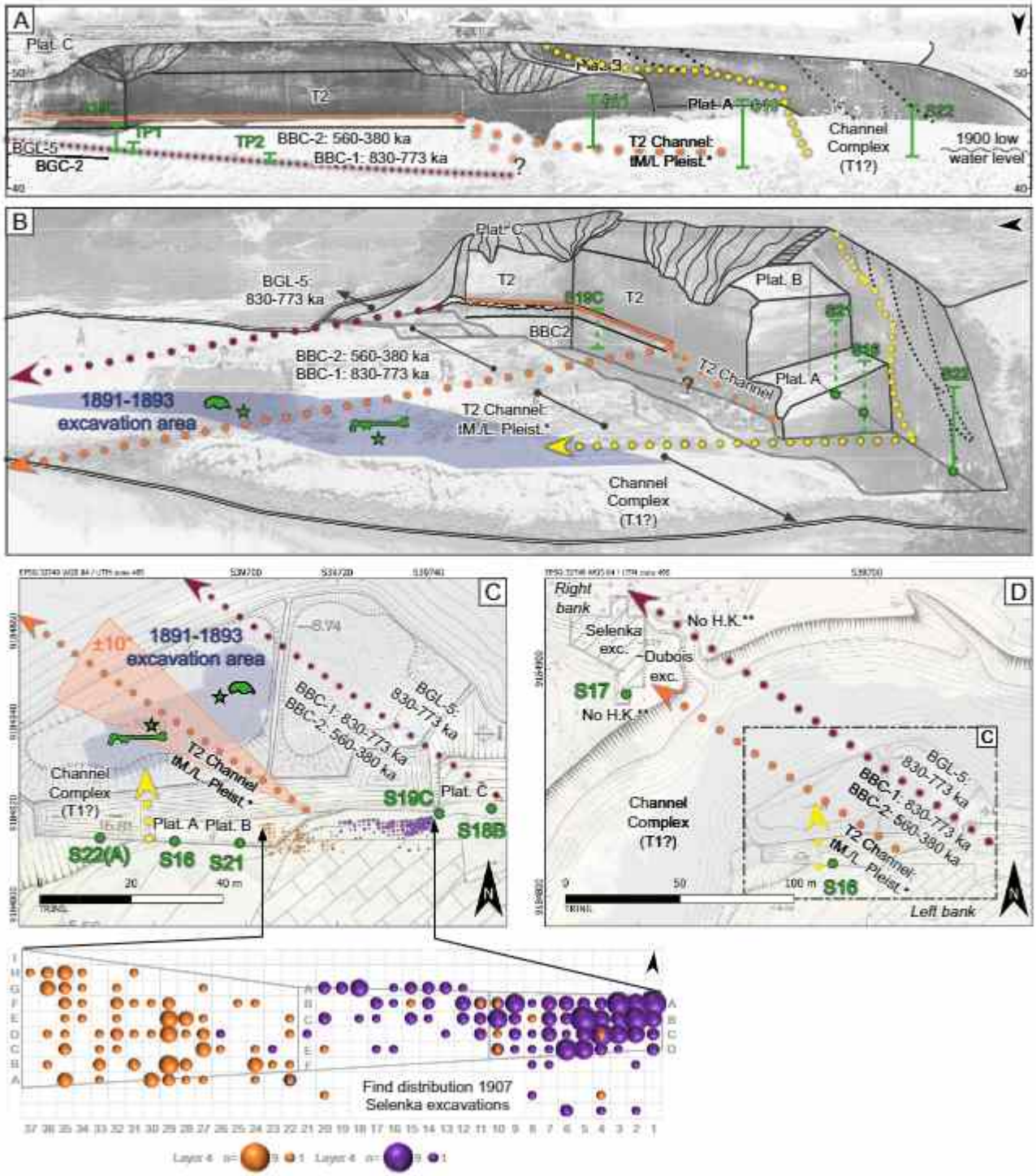

Figure 14. Back wall stratigraphy, channel incisions (and associated ages), and the position of the 2018–2019 sections documenting recurrent fluvial incision at the Trinil site. (**A**) Stratigraphy (including channel incisions) as visible or expected (e.g., below water level) along the 1900 back wall projected on the scaled 1900 photo II with the position of the 2018–2019 sections (and associated ages) indicated. (**B**) As in A, but projected on the 1900 photo III and including reconstructed course of the incisions toward the north/northwest in relation to the 1891–1893 excavation area that yielded the skullcap and Femur L (**C**) 1900 map with the reconstructed courses of channel incisions (with error margin for the T2 channel) in relation to the 1891–1893 excavations, the reconstructed position of the hominin fossils, and the find distribution of the two most fossil-rich layers excavated during the Selenka excavations of 1907 (see SOM S2). (**D**) 1900 map of wider Trinil area with the reconstructed courses of channel incisions extrapolated to the right bank where they intersect the Selenka and Dubois excavation areas. The position of the Selenka excavation area was obtained by georeferencing the adapted Dubois 1900 map (Selenka and Blanckenhorn, 1911: Fig. 6). The position of the Dubois pit is more approximate and based on SOM Fig. S25C. Single asterisks refer to terminal Middle to Late Pleistocene. Double asterisks indicate observations made during coring (Dozy, 1911a,b). Abbreviation: Plat. = platform.

the east–west section of the 1900 back wall, suggests an orientation roughly perpendicular to the wall. Such a north–south orientation would more or less align with the valley created by the meander belt of the present-day Solo (e.g., Berghuis et al., 2021: Fig. 2A).

In addition, smaller-scale and more recent erosion gullies appear higher in the stratigraphy, sometimes visible in section (see 1907 photo in Fig. 12D), but mostly visible as collapses of their less-consolidated channel infill (see 1894 photo in Fig. 10B and 1900 photo in Fig. 14A–B) or reported as a collapse (in the '24 m pit', Kriele, 1899). The western erosion gully can be traced from 1894 to 1900 images showing a southeast–northwest orientation. This gully is situated too high to have affected the BBC-1/BBC-2 deposits but intersects the level where the *Stegodon* remains were found in during the Selenka excavations (see below).

4.2. Stratigraphic provenance of the fossil remains from Trinil

The combined results of this study and Hilgen et al. (2023) demonstrate that five successive units of different ages are lying at low water levels (i.e., 42.5–45.0 m + MSL) within the area of the historical Trinil excavations: the BGL-5 lahar deposits (830–773 ka), the channel infills of BBC-1 (also 830–773 ka) and BBC-2 (560–380 ka), the T2 channel infill (terminal Middle to Late Pleistocene), and channel complex deposits (potentially related to the T1 terrace, ~31 ka: Berghuis et al., 2021). Together, these deposits span approximately 700 kyr over a distance of a mere 100 m (Fig. 14A).

Based on the study of the historical documentation and the results of the test pits, the BBC-1 and BBC-2 can be identified as the main targets of the historical excavations, although find densities vary horizontally and vertically. The BBC-2 constitutes the key part of the main bone bed (i.e., 'Lapillischicht' or 'Hauptknochenschicht'), while historically, the BBC-1 is sometimes considered a coarse, basal part of the main bone bed, or a separate entity underlying it. The historical excavation pits targeting these deposits clearly terminate where the BBC-1 and BBC-2 wedge out against the fossil-poor BGL-5 deposits in the northeastern part of the excavation area and deepen toward the southwest (see DEM Fig. 10)—i.e., the excavations followed the base of the fossil-rich deposits.

Toward the west of the site, both the BBC-1 and BBC-2 are incised by the substantially younger T2 channel (Fig. 14A–C). Although it was not feasible to investigate the channel infill with test pits (due to a high groundwater table and locally a higher degree of cementation), the sections covering these deposits (S21, S16) did yield fossils, albeit in fairly low quantities. Whether this is representative of the find-density in the deeper-lying parts of the Dubois pits (reaching down to minimally 40.4 +MSL, see Fig. 10), and whether BBC-1/BBC-2 deposits were still situated below the T2 channel remains uncertain (Fig. 14A). The fact that a substantial part of the Dubois excavation area lies within the reconstructed course of the T2 channel suggests that the latter contained sufficient fossils to continue excavating there. The same may hold for the younger channel complex (yielding a vertebrate fossil in S22A and some fossils visible in natural outcrops at similar elevations). It is situated further west, but because of its expected course being more northward than that of the T2 channel, still intersects with substantial parts of Dubois' excavation area (Fig. 14C).

It is noteworthy that Selenka's large-scale excavations of 1907 focused on the eastern side of Dubois' excavation area, except for a small westerly (test) pit (D) that was never expanded (Fig. 6). The find documentation for that year shows that two highly fossiliferous layers were excavated (layer 3 and 4), of which the former can be identified as (a constituent of) the H.K. (SOM S2, SOM Fig. 42). The distributions of finds from both layers do not overlap (Fig. 14C): the easterly one (layer 3/H.K.) aligns with the BBC-1/BBC-2 zone and the westerly one (layer 4) with the reconstructed course of the T2 channel, suggesting that the latter also affected the Selenka excavations. No imagery or other documentation of 1908 is available, but based on post-1908 imagery, platforms A and B appear to have been excavated that year. However, contrary to the Dubois pits in front of it, these excavations never went deeper than –43.5 m as evidenced by primary deposits encountered in S21 and by primary deposits outcropping in front of S16. As work was shifted later in 1908 to the right bank—where almost two times the volume was excavated than at the left bank (Dozy, 1911b)—the decreased prospects at the left bank must have been noted.

Given the high density of fossils in both the BBC-1 and BBC-2 observed during the 2018–2019 fieldwork and the age difference between the two units, together they potentially constitute a large source of heterogeneity within Dubois' and Selenka's left-bank Trinil fossil assemblages. The aforementioned find distribution of the 1907 Selenka excavations suggests that the contribution of the T2 channel may also be significant. Unfortunately, detailed fossil find information is not available for the Dubois excavations but it is clear that they intersected with these channels and that they yielded fossils.

The data presented provide unambiguous evidence for Bartstra's (1982) assertion that terrace deposits can be found at low elevations at Trinil. It also supports his view that Dubois and Selenka (unknowingly) excavated through both older pre-terrace deposits and younger terrace deposits, and that, as a consequence, the Trinil assemblages likely contain fossils of different ages. It should be stressed that the documented cycles of erosion and deposition may have also led to the reworking of older elements in younger layers (see Hilgen et al., 2023). Until there is a way to truly account for the provenance of fossils from the Dubois and Selenka collections (see below), it is thus imperative to consider the Trinil (H.K.) fauna as a mixed one (see Hilgen et al., 2023 for a more elaborate discussion).

All fossils coming from deposits situated above unit 3/4 (orange line in Fig. 14A–B) are of equal or younger age than the T2 channel, including the remains of *Stegodon* and hippopotamus excavated 4–5 m above the BBC-2 during the Selenka campaign.

4.3. The hominin fossils from Trinil

Provenance of the hominin fossils This study established the position of the historical excavation pits, the most likely recovery spots of the key fossils, as well as the approximate orientations of the channels intersecting the historical excavation area. Based on this information, the skullcap, the two molars, and the 1897 premolar can be confidently placed within the zone covered by BBC-1 and BBC-2 deposits (Fig. 14B–C).

For the Trinil Femora II–V, the provenance is difficult to assess. They are reported to have been found during the 1900 excavations (Dubois, 1932a, 1932b, 1934), which covered BBC-1, BBC-2, T2 channel, and younger channel complex deposits (Fig. 14). Their most likely provenance will be further discussed in relation to surface taphonomy below.

To assess the stratigraphic provenance of Femur I, it is necessary to not only know its horizontal position but also know the elevation it was found in, as (1) it is unknown how deep the T2 channel reaches and whether there are BBC-1/BBC-2 deposits still situated below it and (2) the T2 channel gains depth going west as visible on the historical imagery and reflected in the depth at which fine-grained, cross-bedded, fluviatile deposits can be found in sections S16 and S21. Close to where the skullcap was found, the base of the find-bearing deposits sits at a minimum depth of 42.7 m +MSL

(1891 pit on Fig. 8). Dubois' descriptions and (idealized) section drawings indicate that the skullcap (and the most fossil-rich level) was sitting above a ~50 cm thick fossil-bearing conglomerate (e.g., Dubois, 1895b), whose remnants are possibly represented by a stone cover/lag sitting in and around the 1891 pit (Figs. 8, 10). This would situate the skullcap and Femur I—following Dubois' and his assistants' assertions that they were found at the same level (e.g., Kriele and de Winter, 1892d; Dubois, 1894a)—at an elevation of ~43.2 m + MSL, i.e., similar to the water level visible in the 1900 imagery (Fig. 14B). According to a note by Dubois (1893c), the deepest point of the 1893 pit sat 2.8 m below the level of the skullcap (and thus Femur I). If that is subtracted from the 43.2 m estimation for the skullcap, the deepest point of the 1893 pit should be 40.4 m +MSL. This closely approximates the lowest bathymetry point obtained for that pit at 40.55 m +MSL. The elevation of ~43.2 m should be interpreted as a minimum, however, as high fossil densities similar to those described by Dubois could be documented up to elevations of 44.1 m + MSL for BBC-2 deposits in TP1 (SOM Fig. S41). Given these elevations, and whilst acknowledging the uncertainties that are inherent to this type of analysis, at an elevation of >43.2 m + MSL, there is a high probability that the T2 channel intersected the discovery location of Femur I. However, given its sharp incision angle and northward course, it cannot be excluded that also the younger channel complex intersected the discovery location of Femur I (Fig. 14B–C).

These findings make it worthwhile to consider the circumstances surrounding the discovery of Femur I. The exposure that yielded the femur was initially isolated from the 1891 excavations (Dubois, 1892c), relatively small compared to larger-sized trench in which it was later that year incorporated (see section 3.3), and the fossil-rich zone was frequently plagued by floodings (Kriele and de Winter, 1892b, 1892c, 1892e, 1892f)—complicating clear stratigraphic observations. The provenance of the femur was specified by Kriele and de Winter only after Dubois received the shipment that contained the fossil at Tulung Agung (100 km southeast of Trinil) and realized its hominin nature (Dubois 1940). Based on these letters, he concluded that the skullcap and Femur I were coming from the same bed (Dubois, 1940), while the letters outlining its provenance only stated they were coming from (approximately) the same level ('ongeveert op de diepte van de chimpansekop' [the femur]; Kriele and de Winter, 1892d: 1; 'op dezelfde diepte'; Kriele and de Winter, 1892b: 1).

The reconstructed provenance of the hominin fossils presented here is clearly at odds with a recent paper that primarily relied on historical sources (Huffman et al., 2022) and was published when this one was in its revision stage.

Taphonomical considerations Preliminary comparative taphonomical and micro-CT scanning analyses of the hominin fossils from Trinil (Pop et al., 2020) indicate that even though the skullcap and all femora appear to be heavily fossilized, all but Femur I show conspicuous 'pitting' visible on the surface of the bone—possibly due to acid corrosion by pyrite decay (i.e., oxidation). Although the fossil material excavated from the test pits is not necessarily taphonomically representative of the material excavated during the historical excavations and limited to BBC-1 and BBC-2 deposits only, the presence of pitting on the cortical surfaces of most bones is noteworthy, especially compared to fossils with better-preserved surfaces that were encountered in other strata (e.g., the bovid vertebrae from S16). Based on these preliminary results, it is plausible that Femora II–V were—like the skullcap and molars—recovered from BBC-2 or BBC-1 deposits. Although well-preserved fossils like Femur I (i.e., heavily fossilized, but without the pitting observed on BBC-1 and BBC-2 fossils) were recovered from T2 and younger channel deposits, their number is insufficient for a representative comparison. Nevertheless, the appearance of Femur I is strikingly different from the fossils recovered from BBC-1 and BBC-2, with even the fine details of the exostosis on this fossil being preserved. The provenance and (preliminary) taphonomical studies seem to agree with chemical analyses of interior compact bone, that grouped Femora II–V with the skullcap, while Femur I clearly diverged (Bartsiokas and Day, 1993).

Detailed taphonomic studies in the future may shed more light on the provenance of the hominin and non-hominin fossils in the historical collections, but this would require taphonomic reference data based on a sufficiently-large assemblage of material with known provenance. For the Dubois collection, contextual information is rare and, when available, difficult to place within the stratigraphic framework. As mentioned above, the Selenka field data does include stratigraphic provenance information, of which particularly the aforementioned material from layers 3 and 4 provide an interesting research perspective. The fossil assemblage excavated from the 2018–2019 test pits is small and because it has been situated quite close to the surface since the overburden was removed during historical excavations, it is possibly not taphonomically representative of the material excavated by Dubois and Selenka.

The possible age of the Trinil fossils and the current framework of human evolution in Southeast Asia While crucial, knowing the stratigraphic position and the age of these strata is insufficient to assess the actual age of fossils found within them. As outlined in more detail by Hilgen et al. (2023), the erosional and intersectional character of the channel structures, the fluvial character of their find-bearing deposits, as well as the long 'tails' observed in single-grain detrital $^{40}Ar/^{39}Ar$ dating samples—representing almost continuous volcanic activity over the complete span of the Pleistocene—, indicate a large degree of reworking of sediments and, potentially, fossils. This would explain why a 'Trinil H.K. fauna'—which at Trinil is largely situated in deposits of 830–773 and 560–380 ka (Hilgen et al., 2023)—was recovered at the Sangiran site from the fine-grained upper Sangiran Formation up to the 900 ka old Grenzbank (de Vos et al., 1994). This not only constitutes a key problem for the biostratigraphy of Java, which is given further consideration in Hilgen et al. (2023), but also affects the hominin remains from Trinil, as discussed in more detail below.

The skullcap, molars, and 1897 premolar were most likely recovered from BBC-1 and/or BBC-2 deposits of 830–773 or 560–380 ka. However, the morphological studies generally group the Trinil skullcap with Early Pleistocene *H. erectus* fossils from Sangiran (Kaifu et al., 2008, 2015; Baab and Zaim, 2017)—in some cases particularly with the group found in and below the Grenzbank (Kaifu et al., 2011) at >900 ka (Matsu'ura et al., 2020; Hilgen et al., 2022)—but not with Late Pleistocene *H. erectus* from Ngandong (Rizal et al., 2020) or those considered to be of similar (Baab and Zaim, 2017) or intermediate age and/or morphology (Ngawi/Sambungmacan; Baba et al., 2003; Kaifu et al., 2015). Similarly, the two Trinil molars that have been attributed to *H. erectus* by some authors (Smith et al., 2009; Noerwidi et al., 2020) are by others attributed to a non-hominin primate (Schwartz and Tattersall, 2003) or to *Meganthropus palaeojavanicus*, a non-*Homo* hominid for which all other attributed dental remains of known stratigraphic provenance are coming from Early Pleistocene deposits at Sangiran (Zanolli et al., 2019). These results imply that the skullcap and molars were part of an older fauna reworked from BBC-1 (830–773 ka) or even older deposits, as also suggested above.

Femora II–V, for which a BBC-1 and/or BBC-2 provenance is most likely too, were from their 'discovery' onward considered to be morphologically comparable to *H. erectus* femora from Zhoukoudian in China (von Koenigswald and Weidenreich, 1939), while later, some authors have noted similarities with modern humans too (Day and Molleson, 1973; Kennedy, 1983). A recent detailed

morphological study (including CT analysis) concluded that Femora II–V differ significantly from Femur I (discussed below) and are morphologically consistent with Early or early Middle Pleistocene *H. erectus* (Ruff et al., 2015). However, due to the effect of reworking, their age is uncertain and their position in the evolutionary framework of Southeast Asia remains unclear. Direct dating using U-series (e.g., Mijares et al., 2010; Ruff et al., 2022) could provide minimum ages for these key fossils.

Femur I, the 'bone of contention', most likely originates from either T2 channel deposits (terminal Middle to Late Pleistocene) or the younger channel complex whose infill may be as young as ~31 ka (terrace T1; Berghuis et al., 2021; Ruff et al., 2022). Although it cannot be excluded that Femur I was reworked from older deposits too, its surface taphonomy, complete state (which is rare in BBC-2 deposits as documented during recent fieldwork), and relatively modern appearance suggests that it may actually be contemporaneous with the sediments it was most likely deposited in—just like the well-preserved and articulated bovid vertebrae found in S16. Assuming a T2 or T1 age, there are three possibilities for the taxonomic attribution of Femur I. The first is that Femur I—given its possible contemporaneity with the Ngandong fossils—belongs to the youngest group of *H. erectus* that may have persisted on Java as late as ~100 ka (Rizal et al., 2020). Although Femur I is morphologically distinct from Early Pleistocene *H. erectus*, no Javanese late Middle to Late Pleistocene femora are known from a secure stratigraphic context that could be compared against. A new femur from Banjarejo—said to show morphological affinities with both *H. erectus* and *H. sapiens* (Noerwidi et al., 2021)—may offer new possibilities for comparison, but unfortunately lacks a stratigraphic context.

The second possibility is that Femur I belongs to *H. sapiens*. Assuming a T2 age (terminal Middle to Late Pleistocene), it would, however, be the oldest modern human fossil known so far from Southeast Asia, as the earliest proposed *H. sapiens* remains currently postdate ~75 ka in Southeast Asia and Australia (Clarkson et al., 2017; Westaway et al., 2017; Shackelford et al., 2018), while others dispute these claims and maintain a more conservative dispersal date of 50–55 ka (O'Connell et al., 2018; Hublin, 2021). Alternatively, Femur I could derive from the younger channel complex, whose deposits may correlate with the 31 ka old T1 terrace of the Solo Formation (Berghuis et al., 2021). Although Pleistocene modern human fossils are relatively rare in island Southeast Asia, fossils of similar or somewhat older age are known from the area—including a femur from Niah Cave (Borneo; Storm et al., 2013; Curnoe et al., 2016), and further east in Australia (Thorne et al., 1999; Clarkson et al., 2017). In addition, recently two hominin fossil femora from Trinil—T9 and T10—have been sourced to terrace T1 deposits and dated by U-series yielding a minimum age of 31–34 ka (Ruff et al., 2022). These fossils—that were found by Prof. Teuku Jacob in 1978 at the right bank in cross-bedded sands at Trinil—could be identified as a small-bodied *H. sapiens* morphologically aligning with specimens from the late Late Pleistocene, while Femur I aligns with early Late Pleistocene *H. sapiens* (Ruff et al., 2015, 2022).

Third, the inferred relatively young age of Femur I suggests that it could represent a Denisovan individual. The fossil finds from Denisova Cave (Altai, Russia) and Baishiya Cave (Tibetan Plateau, China) and DNA analysis performed on them provide evidence for another hominin present in Asia during the late Middle and Late Pleistocene (e.g., Krause et al., 2010; Chen et al., 2019). Unfortunately, the number of fossils from these sites is small and/or non-diagnostic (Brown et al., 2022) and does not include a femur for comparison. Based on Denisovan introgression in the genomes of present-day populations from Island Southeast Asia and Oceania (Reich et al., 2011; Jacobs et al., 2019; Larena et al., 2021; Teixeira et al., 2021), it has been suggested that Denisovans were present in Southeast Asia (Westaway, 2019) and preliminary morphological comparisons even point to Java (Viola et al., 2019). The recent find of a fossil molar from Laos appears to confirm Denisovan presence in Southeast Asia (Demeter et al., 2022).

The taxonomic uncertainty surrounding Femur I and the provisional status of its youngest possible age, warrant attempts to date the younger channel complex deposits (i.e., S22A) and to directly date the fossil itself using U-series (conform Ruff et al., 2022) and possibly ^{14}C. A paleoproteomics analysis (see e.g., Welker, 2018) of Femur I may reveal the taxonomic identity of this famous thighbone that gave *H. erectus* its species name. The attribution of Femur I to something other than *H. erectus* will have no taxonomic consequences for the latter species, as the skullcap is its type specimen and lectotype (Meikle and Parker, 1994).

4.4. Beyond Trinil

The Trinil excavations played a stimulating role in the development of paleoanthropological fieldwork, showing that dedicated attempts to recover early human fossils could yield spectacular results. However, as demonstrated here, major erosional features were missed, leading to erroneous interpretations regarding the provenance of some of the key fossils. The reasons for this lay partly outside the control of Dubois and his team: the stratigraphy at Trinil is complex, most fossils were found near water level, and the fields of paleoanthropology and sedimentology still stood in their infancy. However, it is fair to say that some of his contemporaries (e.g., members of the Selenka expedition) were more careful in their documentation of the context of their finds than Dubois. For these reasons, as well as the high stakes involved, one should be careful in taking the results and interpretations from this and other early fieldwork in the region at face value (see also Berghuis et al., 2022). In the past, it has been claimed that "doubting the accuracy and care with which Dubois carried out his excavations (…) decreases the value of the famous collection and frustrates the paleontological and biostratigraphic research in S.E. Asia" (Sondaar et al., 1983: 339). All evidence, whether gathered over a century ago by Dubois—who played without a doubt a crucial role in the field of paleoanthropology—or by means of high-tech excavations in the present day, should be met with scrutiny. Such critical interrogation of the evidence determines the value of the information—which in this case includes the collection—and brings true progress for paleontological and biostratigraphic research in Southeast Asia.

5. Conclusions

In this study, the location of the historical Trinil excavations pits and the position of the hominin fossils within them—including Trinil Femur I, the 'bone of contention'—was reconstructed, and the historical stratigraphy was compared and integrated with the results obtained in the 2018–2019 fieldwork. In conjunction with the results of Hilgen et al. (2023), the following conclusions can be drawn:

Much of the stratigraphy documented by the excavations of Dubois and Selenka and (part of the) excavations pits they dug can still be identified at Trinil in the present day. However, the Trinil stratigraphy is more complex than previously assumed, with evidence for intermittent fluvial incision and aggradation having taken place at the site, and the presence of Early to Late Pleistocene fossiliferous deposits situated at low water level.

The BBC-1 (830–773 ka) and BBC-2 (560–380 ka) channels—that incise and overly the fossil-poor BGL-5 lahar—can be identified as the primary targets of the historical Dubois and Selenka excavations. As they are both highly fossiliferous, but of very different

ages, they are likely to constitute a large source of heterogeneity within Dubois' and Selenka's fossil assemblages.

The skullcap, molars, and Femora II–V likely originate from the BBC-1 and BBC-2 channel infills, but reworking from older layers is likely.

The T2 channel (terminal Middle to Late Pleistocene) incised the BBC-1 and BBC-2 deposits and ran in a southeast–northwest orientation through large parts of the historical excavation area. A younger channel complex (possibly T1 at ~31 ka) is likely to have intersected large parts of the Dubois excavation area as well. Both the reconstructed course of the T2 channel and that of the younger channel complex intersect the reconstructed discovery location of Femur I. Of course, the exact course of the channel between the control points on the left and right bank cannot be established anymore, but the reconstructions provide a plausible explanation for the difference in the morphology, taphonomy, and earlier chemical analyses of Femur I in comparison with the skullcap and Femur II–V. It undermines the credibility of a scenario in which the skullcap and femur were recovered from the same stratigraphic layer and places the burden of proof on potential proponents of that hypothesis.

Given the morphology and two most likely ages for Femur I, it may belong to *H. erectus* (c.f. Ngandong), to *H. sapiens*, or possibly to a Denisovan. Dating of deposits exposed in the westernmost part of the Trinil site, direct dating of Femur I, and proteomics will shed more light on its provenance, age, and taxonomic position.

The Trinil site as a case study underlines the challenges of working with historical collections/sites, particularly when they are situated in complex, fluvial contexts. Although new fieldwork at such sites can address most existing issues, however, certain issues inherent to fluvially reworked assemblages will remain uncertain. New fieldwork within fine-grained (basin) contexts may offer the best way forward.

Declaration of competing interest

No conflict of interest.

Acknowledgments

This study was carried out with permission of the Indonesian Ministry of Research, Technology and Higher Education (RISTEK research permits: 263/SIP/FRP/ES/Dit.KI/VII/2016, 33/SIP/FRP/E5/Dit.KI/II/2018, and 12/E5/E5.4/SIP.EXT/2019 to J.J.; 2883/FRP/E5/Dit.KI/VIII/2018 and 13/E5/E5.4/SIP.EXT/2019 to E.P.) under the project 'Studying Human Origin in East Java'. We thank Arkenas (Pusat Penelitian Arkeologi Nasional) and in particular I Made Geria, Priyatno Hadi Sulistyarto, and Marlon Ririmasse for the pleasant research collaboration. We are grateful to the people of Trinil and the staff of the Trinil Museum for their hospitality and support. We thank our 2016, 2018, and 2019 fieldwork teams, notably our collaborators and assistants Catur Hari Gumono, Agus Hadi Widianto, Suwono, and their team, and the research team of the Sangiran Museum and the students from Gadjah Mada University in Yogyakarta. We thank Frank Huffman for providing in 2019 unpublished analyses of the 1891–1908 excavations. Thomas Schossleitner (Museum für Naturkunde, Berlin) is acknowledged for photographing the 1907 Selenka map and making the Selenka Collection documentation available to us, Yann Dogger for assistance with the trigonometry used in the sightline intersection analysis, and Natasja den Ouden and Karien Lahaise for assistance with the archival material of the Dubois collection. Finally, we would like to thank the Editor-in-Chief and the reviewers for their useful comments. The research was funded by the Treub Foundation (Maatschappij voor Wetenschappelijk Onderzoek in de Tropen), SNMAP (Stichting Nederlands Museum voor Anthropologie en Praehistorie), the Faculty of Archaeology, Leiden University and the Dutch Research Council NWO (Grant number 016.Vidi.171.049).

Supplementary Online Material

Supplementary Online Material to this article can be found online at https://doi.org/10.1016/j.jhevol.2022.103312.

References

Albers, P.C., De Vos, J., 2010. Through Eugène Dubois' Eyes: Stills of a Turbulent Life. Brill, Leiden. https://doi.org/10.1163/ej.9789004183001.i-186.

Alken, P., Thébault, E., Beggan, C.D., Amit, H., Aubert, J., Baerenzung, J., Bondar, T.N., Brown, W.J., Califf, S., Chambodut, A., Chulliat, A., Cox, G.A., Finlay, C.C., Fournier, A., Gillet, N., Grayver, A., Hammer, M.D., Holschneider, M., Huder, L., Hulot, G., Jager, T., Kloss, C., Korte, M., Kuang, W., Kuvshinov, A., Langlais, B., Léger, J.-M., Lesur, V., Livermore, P.W., Lowes, F.J., Macmillan, S., Magnes, W., Mandea, M., Marsal, S., Matzka, J., Metman, M.C., Minami, T., Morschhauser, A., Mound, J.E., Nair, M., Nakano, S., Olsen, N., Pavón-Carrasco, F.J., Petrov, V.G., Ropp, G., Rother, M., Sabaka, T.J., Sanchez, S., Saturnino, D., Schnepf, N.R., Shen, X., Stolle, C., Tangborn, A., Tøffner-Clausen, L., Toh, H., Torta, J.M., Varner, J., Vervelidou, F., Vigneron, P., Wardinski, I., Wicht, J., Woods, A., Yang, Y., Zeren, Z., Zhou, B., 2021. International Geomagnetic Reference Field: The thirteenth generation. Earth Planets Space 73, 49. https://doi.org/10.1186/s40623-020-01288-x.

Baab, K.L., Zaim, Y., 2017. Global and local perspectives on cranial shape variation in Indonesian *Homo erectus*. Anthropol. Sci. 125, 67–83. https://doi.org/10.1537/ase.170413.

Baba, H., Aziz, F., Kaifu, Y., Suwa, G., Kono, R.T., Jacob, T., 2003. *Homo erectus* calvarium from the Pleistocene of Java. Science 299, 1384–1388. https://doi.org/10.1126/science.1081676.

Bartsiokas, A., Day, M.H., 1993. Electron probe energy dispersive X-ray microanalysis (EDXA) in the investigation of fossil bone: The case of Java Man. Proc. R. Soc. B 252, 115–123. https://doi.org/10.1098/rspb.1993.0054.

Bartstra, G.J., 1982. The river-laid strata near Trinil, site of *Homo erectus erectus*, Java, Indonesia. In: Bartstra, G.J., Casparie, W.A. (Eds.), Modern Quaternary Research in Southeast Asia 7. Balkema, Rotterdam, pp. 97–130.

Bartstra, G.J., 1983. Comment I: The vertebrate-bearing deposits of Kedungbrubus and Trinil, Java, Indonesia. Comments and reply on: The fauna from Trinil, type locality of *Homo erectus*: A reinterpretation. Geol. Mijnbouw 62, 329–336.

Beck, L.A., Joger, U. (Eds.), 2018. Paleontological Collections of Germany, Austria and Switzerland: The History of Life of Fossil Organisms at Museums and Universities. Springer International Publishing, Cham. https://doi.org/10.1007/978-3-319-77401-5.

Berghuis, H.W.K., Veldkamp, A., Adhityatama, S., Hilgen, S.J., Sutisna, I., Barianto, D.H., Pop, E.A.L., Reimann, T., Yurnaldi, D., Ekowati, D.R., Vonhof, H.B., van Kolfschoten, T., Simanjuntak, T., Schoorl, J.M., Joordens, J.C.A., 2021. Hominin homelands of East Java: Revised stratigraphy and landscape reconstructions for Plio-Pleistocene Trinil. Quat. Sci. Rev. 260, 106912. https://doi.org/10.1016/j.quascirev.2021.106912.

Berghuis, H.W.K., van Kolfschoten, T., Adhityatama, S., Troelstra, S.R., Noerwidi, S., Suriyanto, R.A., Wibowo, U.P., Pop, E., Kurniawan, I., Hilgen, S.J., Veldkamp, A., Joordens, J.C.A., 2022. The eastern Kendeng Hills (Java, Indonesia) and the hominin-bearing beds of Mojokerto, a re-interpretation. Quat. Sci. Rev. 295, 107692. https://doi.org/10.1016/j.quascirev.2022.107692.

Bergman, R.A.M., Karsten, P., 1952. The fluorine content of Pithecanthropus and of other specimens from the Trinil fauna. Proc. K. Ned. Akad. Wet. Amst. 54, 150–151.

Brown, S., Massilani, D., Kozlikin, M.B., Shunkov, M.V., Derevianko, A.P., Stoessel, A., Jope-Street, B., Meyer, M., Kelso, J., Pääbo, S., Higham, T., Douka, K., 2022. The earliest Denisovans and their cultural adaptation. Nat. Ecol. Evol. 6, 28–35. https://doi.org/10.1038/s41559-021-01581-2.

Carthaus, E., 1911a. Zur Geologie von Java. In: Selenka, L., Blanckenhorn, M. (Eds.), Die *Pithecanthropus*-Schichten auf Java. Geologische und Paläontologische Ergebnisse der Trinil-Expedition (1907 und 1908). W. Engelmann, Leipzig. https://doi.org/10.5962/bhl.title.60936.

Carthaus, E., 1911b. Arbeitsbericht über die Ausgrabungen. II. Teil. Die Arbeiten von August bis November 1907. In: Selenka, L., Blanckenhorn, M. (Eds.), Die *Pithecanthropus*-Schichten auf Java. Geologische und Paläontologische Ergebnisse der Trinil-Expedition (1907 und 1908). W. Engelmann, Leipzig pp. XXXVIII–XXXIX. https://doi.org/10.5962/bhl.title.60936.

Chen, F., Welker, F., Shen, C.-C., Bailey, S.E., Bergmann, I., Davis, S., Xia, H., Wang, H., Fischer, R., Freidline, S.E., Yu, T.-L., Skinner, M.M., Stelzer, S., Dong, Guangrong, Fu, Q., Dong, Guanghui, Wang, J., Zhang, D., Hublin, J.-J., 2019. A late Middle Pleistocene Denisovan mandible from the Tibetan Plateau. Nature 569, 409–412. https://doi.org/10.1038/s41586-019-1139-x.

Clarkson, C., Jacobs, Z., Marwick, B., Fullagar, R., Wallis, L., Smith, M., Roberts, R.G., Hayes, E., Lowe, K., Carah, X., Florin, S.A., McNeil, J., Cox, D., Arnold, L.J., Hua, Q., Huntley, J., Brand, H.E.A., Manne, T., Fairbairn, A., Shulmeister, J., Lyle, L.,

Salinas, M., Page, M., Connell, K., Park, G., Norman, K., Murphy, T., Pardoe, C., 2017. Human occupation of northern Australia by 65,000 years ago. Nature 547, 306–310. https://doi.org/10.1038/nature22968.
Cunningham, D.J., 1895. Dr. Dubois' so-called missing link. Nature 51, 428–429. https://doi.org/10.1038/051428a0.
Curnoe, D., Datan, I., Taçon, P.S.C., Leh Moi Ung, C., Sauffi, M.S., 2016. Deep skull from Niah Cave and the Pleistocene peopling of Southeast Asia. Front. Ecol. Evol. 4, 75. https://doi.org/10.3389/fevo.2016.00075.
Day, M.H., Molleson, T.I., 1973. The Trinil femora. In: Day, M.H. (Ed.), Human Evolution, Symposia of the Society for the Study of Human Biology. Taylor & Francis, London, pp. 127–154.
Day, M.H., 1984. The postcranial remains of *Homo erectus* from Africa, Asia and possibly Europe. Cour. Forsch.-Inst. Senckenberg 69, 113–121.
Day, M.H., 1986a. Bipedalism: Pressures, origins and modes. In: Wood, B., Martin, L., Andrews, P. (Eds.), Major Topics in Human Evolution. Cambridge University Press, Cambridge, pp. 188–202.
Day, M.H., 1986b. *Homo erectus*: An old species with new problems. Bull. Soc. Roy. Belge Anthrop. Prehist. 97, 33–44.
Demeter, F., Zanolli, C., Westaway, K.E., Joannes-Boyau, R., Duringer, P., Morley, M.W., Welker, F., Rüther, P.L., Skinner, M.M., McColl, H., Gaunitz, C., Vinner, L., Dunn, T.E., Olsen, J.V., Sikora, M., Ponche, J.-L., Suzzoni, E., Frangeul, S., Boesch, Q., Antoine, P.-O., Pan, L., Xing, S., Zhao, J.-X., Bailey, R.M., Boualaphane, S., Sichanthongtip, P., Sihanam, D., Patole-Edoumba, E., Aubaile, F., Crozier, F., Bourgon, N., Zachwieja, A., Luangkhoth, T., Souksavatdy, V., Sayavongkhamdy, T., Cappellini, E., Bacon, A.-M., Hublin, J.-J., Willerslev, E., Shackelford, L., 2022. A Middle Pleistocene Denisovan molar from the Annamite Chain of northern Laos. Nat. Commun. 13, 2557.
de Vos, J., Aziz, F., 1989. The Excavations by Dubois (1891–1900), Selenka (1906–1908), and the Geological Survey by the Indonesian-Japanese Team (1976–1977) at Trinil (Java, Indonesia). J. Anthropol. Soc. Nippon 97, 407–420. https://doi.org/10.1537/ase1911.97.407.
de Vos, J., Sartono, S., Hardja-Sasmita, S., Sondaar, P.Y., 1982. The fauna from Trinil, type locality of *Homo erectus*: A reinterpretation. Geol. Mijnbouw 61, 207–211.
de Vos, J., Sondaar, P.Y., 1982. The importance of the "Dubois Collection" reconsidered. In: Bartstra, G.J., Casparie, W.A. (Eds.), Modern Quaternary Research in Southeast Asia 7. Balkema, Rotterdam, pp. 35–63.
de Vos, J., Sondaar, P.Y., van den Bergh, G.D., Aziz, F., 1994. The *Homo erectus* deposits of Java and its ecological context. Cour. Forsch.-Inst. Senckenberg 171, 129–140.
Dozy, C.M., 1909. De opgravingen bij Trinil in 1908. Tijdschr. Kon. Nederl. Aardrijks. Genoot. XXVI, 604–611.
Dozy, C.M., 1911a. Bemerkungen zu Stratigraphie der Sedimente in der Triniler Gegend. In: Selenka, L., Blanckenhorn, M. (Eds.), Die *Pithecanthropus*-Schichten auf Java. Geologische und Paläontologische Ergebnisse der Trinil-Expedition (1907 und 1908). W. Engelmann, Leipzig, pp. 34–36. https://doi.org/10.5962/bhl.title.60936.
Dozy, C.M., 1911b. Arbeitsbericht über die Ausgrabungen. III. Teil. Die Arbeiten im Jahre 1908. In: Selenka, L., Blanckenhorn, M. (Eds.), Die *Pithecanthropus*-Schichten auf Java. Geologische und Paläontologische Ergebnisse der Trinil-Expedition (1907 und 1908). W. Engelmann, Leipzig pp. XL–XLII. https://doi.org/10.5962/bhl.title.60936.
Dubois, E., 1892a. Palaeontologische onderzoekingen op Java. Extra bijvoegsel der Javasche Courant, Verslag van het Mijnwezen over het 3e kwartaal 1891, 12–14.
Dubois, E., 1892b. Palaeontologische onderzoekingen op Java. Extra bijvoegsel der Javasche Courant, Verslag van het Mijnwezen over het 4e kwartaal 1891, 12–15.
Dubois, E., 1892c. September 1892. Rapporten van de Palaeontologische onderzoekingen op Java 1890-1894. Dubois Archive (Unpublished). Naturalis, Leiden.
Dubois, E., 1893a. Palaeontologische onderzoekingen op Java. Extra bijvoegsel der Javasche Courant, Verslag van het Mijnwezen over het 3e kwartaal 1892, 10–14.
Dubois, E., 1893b. Palaeontologische onderzoekingen op Java. Extra bijvoegsel der Javasche Courant, Verslag van het Mijnwezen over het 4e kwartaal 1892, 11–12.
Dubois, E., 1893c. Note of 21/10/1893. Dubois Archive (Unpublished). Naturalis, Leiden.
Dubois, E., 1894a. *Pithecanthropus erectus*: Eine Menschenähnliche Übergangsform aus Java. Landesdruckerei, Batavia.
Dubois, E., 1894b. Palaeontologische onderzoekingen op Java. Extra bijvoegsel der Javasche Courant, Verslag van het Mijnwezen over het 3e kwartaal 1893, 15–17.
Dubois, E., 1895a. Sur le *Pithecanthropus erectus* du Pliocène de Java. Bull. Soc. Belge Geol. Paleontol. Hydrol. 9, 151–160.
Dubois, E., 1895b. *Pithecanthropus erectus*, betrachtet als eine wirkliche Uebergangsform und als Stammform des Menschen. Z. Ethnol. 27, 723–738.
Dubois, E., 1895c. *Pithecanthropus erectus*: eine menschenähnliche Übergangsform aus Java. Jaarboek van het Mijnwezen in Nederlandsch-Oost-Indië 24, 1–77.
Dubois, E., 1896a. *Pithecanthropus erectus*: eine menschenaehnliche Uebergangsform. In: Hoek, P.P.C. (Ed.), Compte-Rendu des Séances du Troisième Congrès International de Zoologie Leyde, 11-16 septembre 1895. Brill, Leyde, pp. 251–271.
Dubois, E., 1896b. Le *Pithecanthropus erectus* et l'origine de l'Homme. Bull. Mem. Soc. Anthropol. Paris S4, 460–467. https://doi.org/10.3406/bmsap.1896.5655.
Dubois, E., 1896c. Näheres über den Pithecanthropus erectus als menschenähnliche Uebergangsform. Internationale Monatschrift für Anatomie und Physiologie 13, 1–28.
Dubois, E., 1896d. On *Pithecanthropus erectus*: A transitional form between man and the apes. Sci. Trans. R. Dublin Soc. 2, 1–18.
Dubois, E., 1896e. On *Pithecanthropus erectus*: A transitional form between man and the apes. J. Anthropol. Inst. G. B. Ireland 25, 240–248.
Dubois, E., 1896f. *Pithecanthropus erectus*, eine Stammform des Menschen. Anat. Anzeiger 12, 1–22.
Dubois, E., 1899. Remarks upon the brain cast of Pithecanthropus erectus. In: Sedgwick, A. (Ed.), Proceedings of the Fourth International Congress of Zoology Cambridge 22-27 August 1898. Clay and Sons, London, pp. 78–95. https://doi.org/10.5962/bhl.title.31991.
Dubois, E., 1907. Eenige van Nederlandschen kant verkregen uitkomsten met betrekking tot de kennis der Kendeng-fauna (fauna van Trinil). Tijdschr. Kon. Nederl. Aardrijks. Genoot. 2, 449–458.
Dubois, E., 1908. Das geologische Alter der Kendeng-oder Trinil-fauna. Tijdschr. Kon. Nederl. Aardrijks. Genoot. 2, 1235–1270.
Dubois, E., 1932a. De afzonderlijk organisatie van *Pithecanthropus* waarvan het femur getuigt, thans bevestigd door andere individuen van de beschreven soort. Verslag van de gewone vergaderingen der afdeeling natuurkunde. Proc. K. Ned. Akad. Wet. Amst. 41, 76–77.
Dubois, E., 1932b. The distinct organization of *Pithecanthropus* of which the femur bears evidence, now confirmed from other individuals of the described species. Proc. K. Ned. Akad. Wet. Amst. 35, 716–722.
Dubois, E., 1934. New evidence of the distinct organization of Pithecanthropus. Proc. K. Ned. Akad. Wet. Amst. 37, 139–145.
Duyfjes, J., 1936. Zur Geologie und Stratigraphie des Kendenggebietes zwischen Trinil und Soerabaja (Java). De Ingenieur Ned.-Indie 4, 136–149.
Dubois, E., 1940. Letter to Woendeman 15/02/1940. Dubois Archive (Unpublished). Naturalis, Leiden.
Elbert, J., 1908. Über das Alter der Kendeng-Schichten mit *Pithecanthropus erectus* Dubois. Neues Jahrbuch für Mineralogie, Geologie und Paläontologie XXV, 648–662.
Hepburn, D., 1896. The Trinil femur (*Pithecanthropus erectus*), contrasted with the femora of various savage and civilised races. J. Anat. Physiol. 31, 1–17.
Hilgen, S.L., Hilgen, F.J., Adhityatama, S., Kuiper, K.F., Joordens, J.C.A., 2022. Towards an astronomical age model for the Lower to Middle Pleistocene hominin-bearing succession of the Sangiran Dome area on Java, Indonesia. Quat. Sci. Rev. 297, 107788.
Hilgen, S.L., Pop, E., Adhityatama, S., Veldkamp, A., Berghuis, H.W.K., Sutisna, I., Yurnaldi, D., Dupont-Nivet, G., Reimann, T., Nowaczyk, N., Kuiper, K.F., Krijgsman, W., Vonhof, H.B., Ekowati, D.R., Alink, G., Hafsari, N.L.G.D.M., Drespriputra, O., Verpoorte, A., Bos, R., Simanjuntak, T., Prasetyo, B., Joordens, J.C.A., 2023. Revised age and stratigraphy of the classic *Homo erectus* bearing succession at Trinil (Java, Indonesia). Quat. Sci. Rev. 301, 107908.
Howell, F.C., 1994. Thoughts on Eugène Dubois and the "*Pithecanthropus*" Saga. Cour. Forsch.-Inst. Senckenberg 171, 11–20.
Hrdlicka, A., 1930. The Skeletal Remains of Early Man. Smithsonian Miscellaneous Collections 83. Smithsonian Institution, Washington.
Hublin, J.-J., 2021. How old are the oldest *Homo sapiens* in Far East Asia? Proc. Natl. Acad. Sci. USA 118, e2101173118. https://doi.org/10.1073/pnas.2101173118.
Huffman, F., Berkhout, A.W.J., Albers, P.C.H., de Vos, J., Aziz, F., 2022. Geology and discovery record of the Trinil *Pithecanthropus erectus* site, Java. PaleoAnthropology 2022, 266–326. https://doi.org/10.48738/2022.iss2.83.
Indriati, E., 2004. Indonesian fossil hominid discoveries from 1889-2003: Catalogue and problems. In: Akiyama, S., Miyawaki, R., Kubodera, T., Higuchi, M. (Eds.), Proceedings of the 5th and 6th Symposia on Collection Building and Natural History Studies in Asia and the Pacific Rim. National Science Museum Monographs 24. National Science Museum, Tokyo, pp. 163–172.
Jacobs, G.S., Hudjashov, G., Saag, L., Kusuma, P., Darusallam, C.C., Lawson, D.J., Mondal, M., Pagani, L., Ricaut, F.-X., Stoneking, M., Metspalu, M., Sudoyo, H., Lansing, J.S., Cox, M.P., 2019. Multiple deeply divergent Denisovan ancestries in Papuans. Cell 177, 1010–1021. https://doi.org/10.1016/j.cell.2019.02.035.
Joordens, J.C.A., d'Errico, F., Wesselingh, F.P., Munro, S., de Vos, J., Wallinga, J., Ankjærgaard, C., Reimann, T., Wijbrans, J.R., Kuiper, K.F., Mücher, H.J., Coqueugniot, H., Prié, V., Joosten, I., van Os, B., Schulp, A.S., Panuel, M., van der Haas, V., Lustenhouwer, W., Reijmer, J.J.G., Roebroeks, W., 2015. *Homo erectus* at Trinil on Java used shells for tool production and engraving. Nature 518, 228–231. https://doi.org/10.1038/nature13962.
Kaifu, Y., Aziz, F., Indriati, E., Jacob, T., Kurniawan, I., Baba, H., 2008. Cranial morphology of Javanese *Homo erectus*: New evidence for continuous evolution, specialization, and terminal extinction. J. Hum. Evol. 55, 551–580. https://doi.org/10.1016/j.jhevol.2008.05.002.
Kaifu, Y., Indriati, E., Aziz, F., Kurniawan, I., Baba, H., 2011. Cranial morphology and variation of the earliest Indonesian Hominids. In: Norton, C.J., Braun, D.R. (Eds.), Asian Paleoanthropology: From Africa to China and Beyond, Vertebrate Paleobiology and Paleoanthropology. Springer Netherlands, Dordrecht, pp. 143–157. https://doi.org/10.1007/978-90-481-9094-2.
Kaifu, Y., Kurniawan, I., Kubo, D., Sudiyabudi, E., Putro, G.P., Prasanti, E., Aziz, F., Baba, H., 2015. *Homo erectus* calvaria from Ngawi (Java) and its evolutionary implications. Anthropol. Sci. 123, 161–176. https://doi.org/10.1537/ase.150702.
Kennedy, G.E., 1983. Some aspects of femoral morphology in *Homo erectus*. J. Hum. Evol. 12, 587–616. https://doi.org/10.1016/S0047-2484(83)80001-3.

Krause, J., Fu, Q., Good, J.M., Viola, B., Shunkov, M.V., Derevianko, A.P., Pääbo, S., 2010. The complete mitochondrial DNA genome of an unknown hominin from southern Siberia. Nature 464, 894–897. https://doi.org/10.1038/nature08976.
Kriele, de Winter, 1892a. Letter to E. Dubois 18/11/1892. Dubois Archive (Unpublished). Naturalis, Leiden.
Kriele, de Winter, 1892b. Letter to E. Dubois 7/9/1892. Dubois Archive (Unpublished). Naturalis, Leiden.
Kriele, de Winter, 1892c. Letter to E. Dubois 28/10/1892. Dubois Archive (Unpublished). Naturalis, Leiden.
Kriele, de Winter, 1892d. Letter to E. Dubois 31/8/1892. Dubois Archive (Unpublished). Naturalis, Leiden.
Kriele, de Winter, 1892e. Letter to E. Dubois 15/8/1892. Dubois Archive (Unpublished). Naturalis, Leiden.
Kriele, de Winter, 1892f. Letter to E. Dubois 22/8/1892. Dubois Archive (Unpublished). Naturalis, Leiden.
Kriele, de Winter, 1893. Letter to E. Dubois 14/10/1893. Dubois Archive (Unpublished). Naturalis, Leiden.
Kriele, de Winter, 1895a. Letter to E. Dubois 15/10/1895. Dubois Archive (Unpublished). Naturalis, Leiden.
Kriele, de Winter, 1895b. Letter to E. Dubois, 18/11/1895. In: Dubois Archive (Unpublished). Naturalis, Leiden.
Kriele, de Winter, 1896. Letter to E. Dubois 1/10/1896. Dubois Archive (Unpublished). Naturalis, Leiden.
Kriele, de Winter, 1899. Letter to E. Dubois 7/11/1899. Dubois Archive (Unpublished). Naturalis, Leiden.
Kriele, de Winter, 1900a. Letter to E. Dubois 21/11/1900. Dubois Archive (Unpublished). Naturalis, Leiden.
Kriele, de Winter, 1900b. Letter to E. Dubois 28/4/1900. Dubois Archive (Unpublished). Naturalis, Leiden.
Larena, M., McKenna, J., Sanchez-Quinto, F., Bernhardsson, C., Eheo, C., Reyes, R., Casel, O., Huang, J.-Y., Hagada, K.P., Guilay, D., Reyes, J., Allian, F.P., Mori, V., Azarcon, L.S., Manera, A., Terando, C., Jamero, L., Sireg, G., Manginsay-Tremedal, R., Labos, M.S., Vilar, R.D., Latiph, A., Saway, R.L., Marte, E., Magbanua, P., Morales, A., Java, L., Reveche, R., Barrios, B., Burton, E., Salon, J.C., Kels, M.J.T., Albano, A., Cruz-Angeles, R.B., Molanida, E., Granehäll, L., Vicente, M., Edlund, H., Loo, J.-H., Trejaut, J., Ho, S.Y.W., Reid, L., Lambeck, K., Malmström, H., Schlebusch, C., Endicott, P., Jakobsson, M., 2021. Philippine Ayta possess the highest level of Denisovan ancestry in the world. Curr. Biol. 31, 4219–4230. https://doi.org/10.1016/j.cub.2021.07.022.
Manouvrier, L., 1895. Deuxième étude sur le "Pithecanthropus erectus" comme précurseur présumé de l'homme. Bull. Soc. Anthropol. Paris 6, 554–654. https://doi.org/10.5962/bhl.title.101930.
Matsu'ura, S., 1986. Fluorine and phosphate analysis of fossil bones from the Kabuh Formation of Trinil. Bull. Natl. Sci. Mus. D 12, 1–9.
Matsu'ura, S., Kondo, M., Danhara, T., Sakata, S., Iwano, H., Hirata, T., Kurniawan, I., Setiyabudi, E., Takeshita, Y., Hyodo, M., Kitaba, I., Sudo, M., Danhara, Y., Aziz, F., 2020. Age control of the first appearance datum for Javanese *Homo erectus* in the Sangiran area. Science 367, 210–214. https://doi.org/10.1126/science.aau8556.
Mayr, E., 1944. On the concepts and terminology of vertical subspecies and species. Natl. Res. Council Bull. 2, 11–16.
Mayr, E., 1950. Taxonomic categories in fossil hominids. Cold Spring Harbor Symp. Quant. Biol. 15, 109–118.
Meikle, W.E., Parker, S.T., 1994. Naming Our Ancestors: An Anthology of Hominid Taxonomy. Waveland Pr Inc, Prospect Heights.
Mijares, A.S., Détroit, F., Piper, P., Grün, R., Bellwood, P., Aubert, M., Champion, G., Cuevas, N., De Leon, A., Dizon, E., 2010. New evidence for a 67,000-year-old human presence at Callao Cave, Luzon, Philippines. J. Hum. Evol. 59, 123–132. https://doi.org/10.1016/j.jhevol.2010.04.008.
NOAA, 2020. National Oceanic and Atmospheric Administration. Historical Declination Viewer. https://maps.ngdc.noaa.gov/viewers/historical_declination/. (Accessed 17 December 2021).
Noerwidi, S., Suriyanto, R.A., Prayudi, A., Widianto, H., 2021. Hominin femur finding from Banjarejo: Its morphological character and taxonomical position. Indones. J. Sediment. Geol. 8–16. https://doi.org/10.51835/bsed.2021.47.3.350.
Noerwidi, S., Vialet, A., Widianto, H., Kurniawan, I., Zaim, J., Suriyanto, R.A., Joordens, J., Lorenzo, C., Simanjuntak, T., Sémah, F., 2020. Exploring the diversity of fossil hominin dental patterns in the western Indonesian archipelago during the Quaternary by geometric morphometric analysis. Application on second upper and lower molars. L'Anthropologie 124, 102791. https://doi.org/10.1016/j.anthro.2020.102791.
O'Connell, J.F., Allen, J., Williams, M.A.J., Williams, A.N., Turney, C.S.M., Spooner, N.A., Kamminga, J., Brown, G., Cooper, A., 2018. When did *Homo sapiens* first reach Southeast Asia and Sahul? Proc. Natl. Acad. Sci. USA 115, 8482–8490. https://doi.org/10.1073/pnas.1808385115.
Oppenoorth, F., 1911. Arbeitsbericht über die Ausgrabungen. I. Teil. Die Arbeiten des Jahres 1907 bis August. In: Selenka, L., Blanckenhorn, M. (Eds.), Die *Pithecanthropus*-Schichten auf Java. Geologische und Paläontologische Ergebnisse der Trinil-Expedition (1907 und 1908). W. Engelmann, Leipzig pp. XXVI–XXXVIII. https://doi.org/10.5962/bhl.title.60936.
Oppenoorth, W.F.F., 1932. Een nieuwe fossiele Mensch van Java. Tijdschr. Kon. Nederl. Aardrijks. Genoot. 49, 704–707.
Oppenoorth, W.F.F., 1936. Een prehistorisch cultuurcentrum langs de Solo-rivier. Tijdschr. Kon. Nederl. Aardrijks. Genoot. 53, 399–411.
Pop, E., Adhityatama, S., Hilgen, S., Berghuis, H., Sutisna, I., Kostenko, A., Batenburg, J., Joordens, J.C.A., 2020. Quantitatively studying bone taphonomy of *Homo erectus* fossils from Trinil, Indonesia, using surface texture and CT analyses. In: 16th Nederlands Aardwetenschappelijk Congres. Abstract Book.
Reich, D., Patterson, N., Kircher, M., Delfin, F., Nandineni, M.R., Pugach, I., Ko, A.M.-S., Ko, Y.-C., Jinam, T.A., Phipps, M.E., Saitou, N., Wollstein, A., Kayser, M., Pääbo, S., Stoneking, M., 2011. Denisova admixture and the first modern human dispersals into Southeast Asia and Oceania. Am. J. Hum. Genet. 89, 516–528. https://doi.org/10.1016/j.ajhg.2011.09.005.
Rizal, Y., Westaway, K.E., Zaim, Y., van den Bergh, G.D., Bettis, E.A., Morwood, M.J., Huffman, O.F., Grün, R., Joannes-Boyau, R., Bailey, R.M., Sidarto, Westaway, M.C., Kurniawan, I., Moore, M.W., Storey, M., Aziz, F., Suminto, Zhao, J., Aswan, Sipola, M.E., Larick, R., Zonneveld, J.-P., Scott, R., Putt, S., Ciochon, R.L., 2020. Last appearance of *Homo erectus* at Ngandong, Java, 117,000–108,000 years ago. Nature 577, 381–385. https://doi.org/10.1038/s41586-019-1863-2.
Ruff, C.B., Puymerail, L., Macchiarelli, R., Sipla, J., Ciochon, R.L., 2015. Structure and composition of the Trinil femora: Functional and taxonomic implications. J. Hum. Evol. 80, 147–158. https://doi.org/10.1016/j.jhevol.2014.12.004.
Ruff, C.B., Sylvester, A.D., Rahmawati, N.T., Suriyanto, R.A., Storm, P., Aubert, M., Joannes-Boyau, R., Berghuis, H., Pop, E., Batenburg, K.J., Coban, S.B., Kostenko, A., Noerwidi, S., Renema, W., Adhityatama, S., Joordens, J.C., 2022. Two Late Pleistocene human femora from Trinil, Indonesia: Implications for body size and behavior in Southeast Asia. J. Hum. Evol. 172, 103252. https://doi.org/10.1016/j.jhevol.2022.103252.
Shackelford, L., Demeter, F., Westaway, K., Duringer, P., Ponche, J.-L., Sayavongkhamdy, T., Zhao, J.-X., Barnes, L., Boyon, M., Sichanthongtip, P., Sénégas, F., Patole-Edoumba, E., Coppens, Y., Dumoncel, J., Bacon, A.-M., 2018. Additional evidence for early modern human morphological diversity in Southeast Asia at Tam Pa Ling, Laos. Quat. Int. 466, 93–106. https://doi.org/10.1016/j.quaint.2016.12.002.
Schwartz, J.H., Tattersall, I., 2003. Craniodental morphology of genus *Homo* (Africa and Asia). The Human Fossil Record, vol. 2. Wiley-Liss, New York. https://doi.org/10.1002/0471722715.
Selenka, L., Blanckenhorn, M., 1911. Die *Pithecanthropus*-Schichten auf Java. Geologische und Paläontologische Ergebnisse der Trinil-Expedition (1907 und 1908). W. Engelmann, Leipzig. https://doi.org/10.5962/bhl.title.60936.
Smith, T.M., Olejniczak, A.J., Kupczik, K., Lazzari, V., de Vos, J., Kullmer, O., Schrenk, F., Hublin, J.J., Jacob, T., Tafforeau, P., 2009. Taxonomic assessment of the Trinil molars using non-destructive 3D structural and development analysis. Paleoanthropology 2009, 117–129.
Soeradi, T., Shibasaki, T., Kadar, D., Sudjono, Itihara, M., Kumai, H., Hayashi, T., Furuyama, K., Aziz, F., Siagian, H., Furutani, M., Suminto, Yoshikawa, S., 1985. Geology and stratigraphy of the Trinil area. In: Watanabe, O., Kadar, D. (Eds.), Quaternary Geology of the Hominid Fossil Bearing Formations in Java, Special Publication No. 4. Geological Research and Development Centre, Bandung, pp. 49–53.
Sondaar, P.Y., de Vos, J., Leinders, J.J.M., 1983. Reply: Facts and fiction around the fossil mammals of Java. Geol. Mijnbouw 62, 337–338.
Storm, P., Wood, R., Stringer, C., Bartsiokas, A., de Vos, J., Aubert, M., Kinsley, L., Grün, R., 2013. U-series and radiocarbon analyses of human and faunal remains from Wajak, Indonesia. J. Hum. Evol. 64, 356–365. https://doi.org/10.1016/j.jhevol.2012.11.002.
Teixeira, J.C., Jacobs, G.S., Stringer, C., Tuke, J., Hudjashov, G., Purnomo, G.A., Sudoyo, H., Cox, M.P., Tobler, R., Turney, C.S.M., Cooper, A., Helgen, K.M., 2021. Widespread Denisovan ancestry in Island Southeast Asia but no evidence of substantial super-archaic hominin admixture. Nat. Ecol. Evol. 5, 616–624.
Theunissen, B., 1990. Eugène Dubois and the Ape-Man from Java. Springer Netherlands, Dordrecht. https://doi.org/10.1007/978-94-009-2209-9.
Thorne, A., Grün, R., Mortimer, G., Spooner, N.A., Simpson, J.J., McCulloch, M., Taylor, L., Curnoe, D., 1999. Australia's oldest human remains: Age of the Lake Mungo 3 skeleton. J. Hum. Evol. 36, 591–612. https://doi.org/10.1006/jhev.1999.0305.
van den Bergh, G.D., de Vos, J., Sondaar, P.Y., 2001. The Late Quaternary palaeogeography of mammal evolution in the Indonesian Archipelago. Palaeogeogr. Palaeoclimatol. Palaeoecol. 171, 385–408. https://doi.org/10.1016/S0031-0182(01)00255-3.
Viola, B.T., Gunz, P., Neubauer, S., Slon, V., Kozlikin, M.B., Shunkov, M.V., Meyer, M., Pääbo, S., Derevianko, A.P., 2019. A parietal fragment from Denisova cave. Am. J. Phys. Anthropol. 168, 258. https://doi.org/10.1002/ajpa.23802.
von Koenigswald, G.H.R., 1934. Zur Stratigraphie des Javanischen Pleistocän. De Ingenieur in Nederlandsch-Indië 1, 185–201.
von Koenigswald, G.H.R., 1935. Die fossilen Säugetierfaunen Javas. Proc. K. Ned. Akad. Wet. Amst. 38, 188–198.
von Koenigswald, G.H.R., Weidenreich, F., 1939. The relationship between *Pithecanthropus* and *Sinanthropus*. Nature 144, 926–929. https://doi.org/10.1038/1449260a0.
Welker, F., 2018. Palaeoproteomics for human evolution studies. Quat. Sci. Rev. 190, 137–147. https://doi.org/10.1016/j.quascirev.2018.04.033.
Westaway, K.E., Louys, J., Awe, R.D., Morwood, M.J., Price, G.J., Zhao, J.-x., Aubert, M., Joannes-Boyau, R., Smith, T.M., Skinner, M.M., Compton, T., Bailey, R.M., van den Bergh, G.D., de Vos, J., Pike, A.W.G., Stringer, C., Saptomo, E.W., Rizal, Y., Zaim, J.,

Santoso, W.D., Trihascaryo, A., Kinsley, L., Sulistyanto, B., 2017. An early modern human presence in Sumatra 73,000–63,000 years ago. Nature 548, 322–325. https://doi.org/10.1038/nature23452.

Westaway, M.C., 2019. The first hominin fleet. Nat. Ecol. Evol. 3, 999–1000. https://doi.org/10.1038/s41559-019-0928-9.

Zanolli, C., Kullmer, O., Kelley, J., Bacon, A.-M., Demeter, F., Dumoncel, J., Fiorenza, L., Grine, F.E., Hublin, J.-J., Nguyen, A.T., Nguyen, T.M.H., Pan, L., Schillinger, B., Schrenk, F., Skinner, M.M., Ji, X., Macchiarelli, R., 2019. Evidence for increased hominid diversity in the Early to Middle Pleistocene of Indonesia. Nat. Ecol. Evol. 3, 755–764. https://doi.org/10.1038/s41559-019-0860-z.